Short Course on the Fundamentals of Boundary-layer Wind and Temperature Profiling Using Radar and Acoustic Techniques

February 8-9, 2003

PROFILER OBSERVATIONS, APPLICATIONS, AND ANALYSIS – WEATHER PHENOMENA

Dr. Allen B. White

Cooperative Institute for Research in Environmental Sciences

University of Colorado/NOAA Environmental Technology Laboratory

Boulder, CO

Outline

III. Turbulence Intensity

A. Profiler sampling filters
B. Calculating the TKE eddy dissipation rate
C. Sodar backscatter examples

IV. Weather Phenomena

A. Fronts
B. Low-level jets
C. Precipitation
D. Snow-level monitoring
E. Operational forecasting

Estimating Turbulence Intensity

The Doppler velocity spectrum

The Doppler velocity spectrum (DVS) is the fundamental measurement provided by the wind profiler and Doppler sodar. From the DVS, the Doppler spectral moments are calculated. For the purpose of estimating turbulence intensity, we are interested in the 2nd moment, or Doppler spectral width.

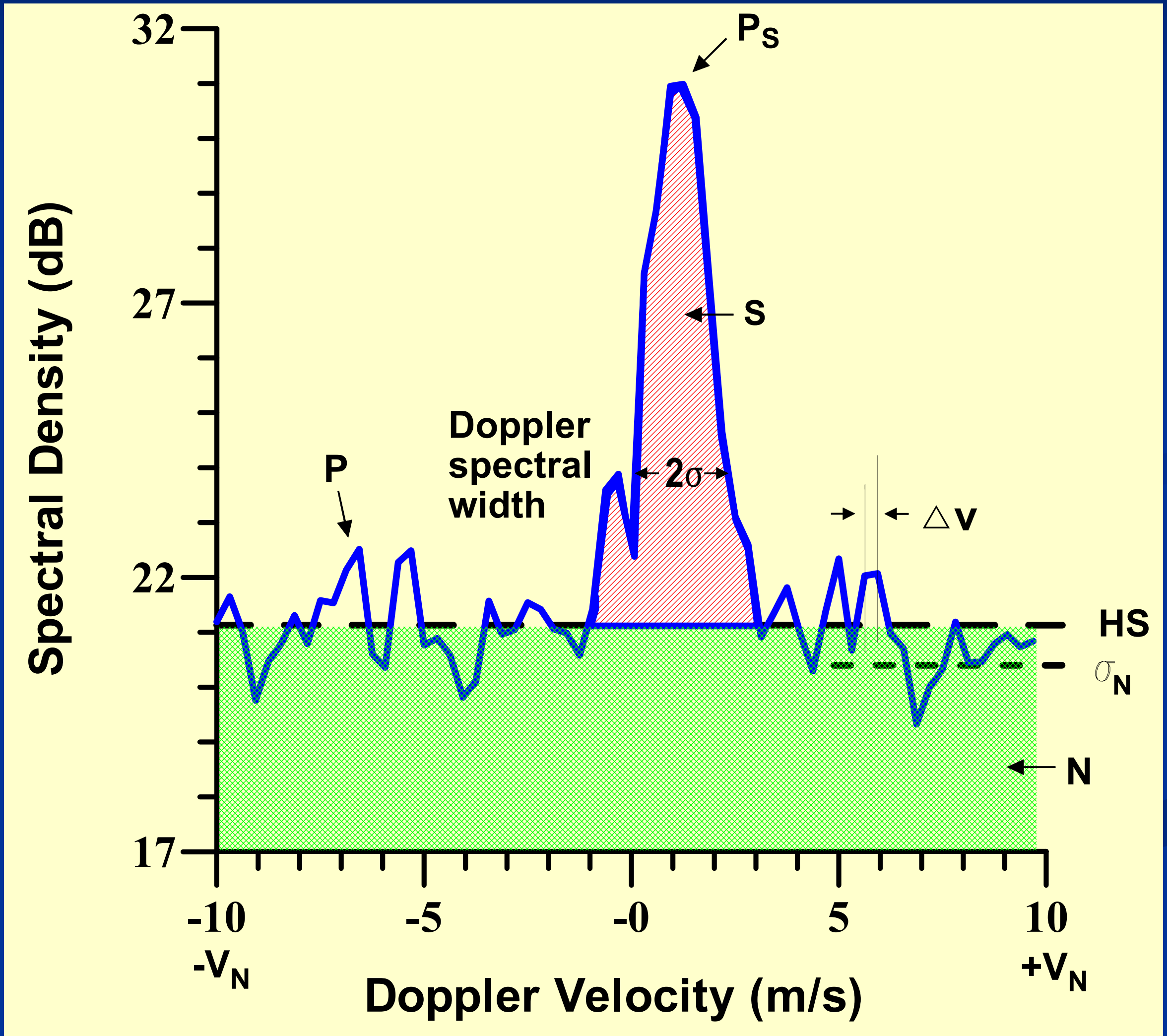

Estimating Turbulence Intensity

Profiler sampling filters

The pulse volume filter and sampling rate filter occur simultaneously within a radar sampling period. These effects must be accounted for when using wind profiler spectral width measurements to estimate turbulence intensity.

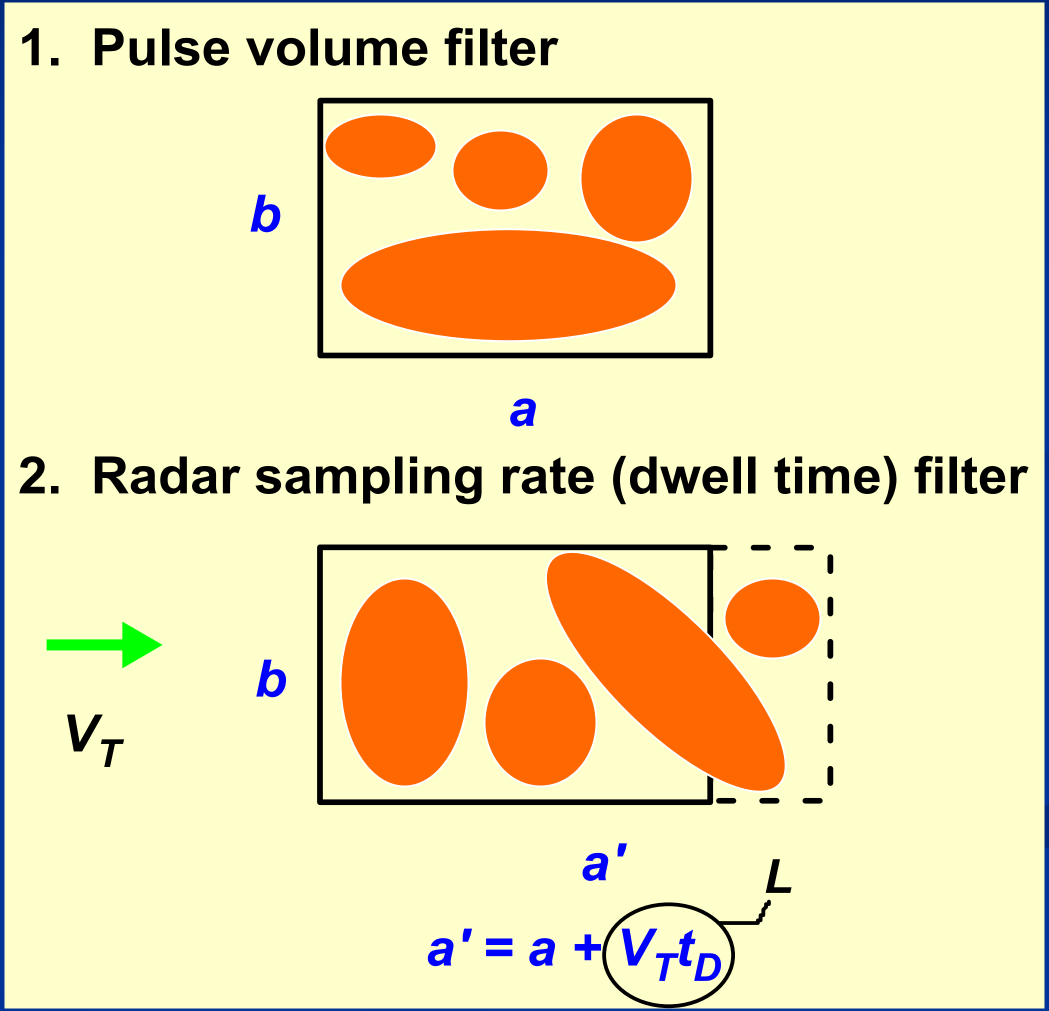

Estimating Turbulence Intensity

Profiler sampling filters

The sonic anemometer measures vertical velocity fluctuations at a high rate (10 Hz in this case) and is, therefore, able to capture the inertial subrange in this normalized vertical velocity power spectrum taken in the CBL at 275 m AGL (z/z_i=0.2). The profiler normalized spectral density falls off because of the temporal and spatial filters inherent to the profiler sampling (dwell time and pulse volume).

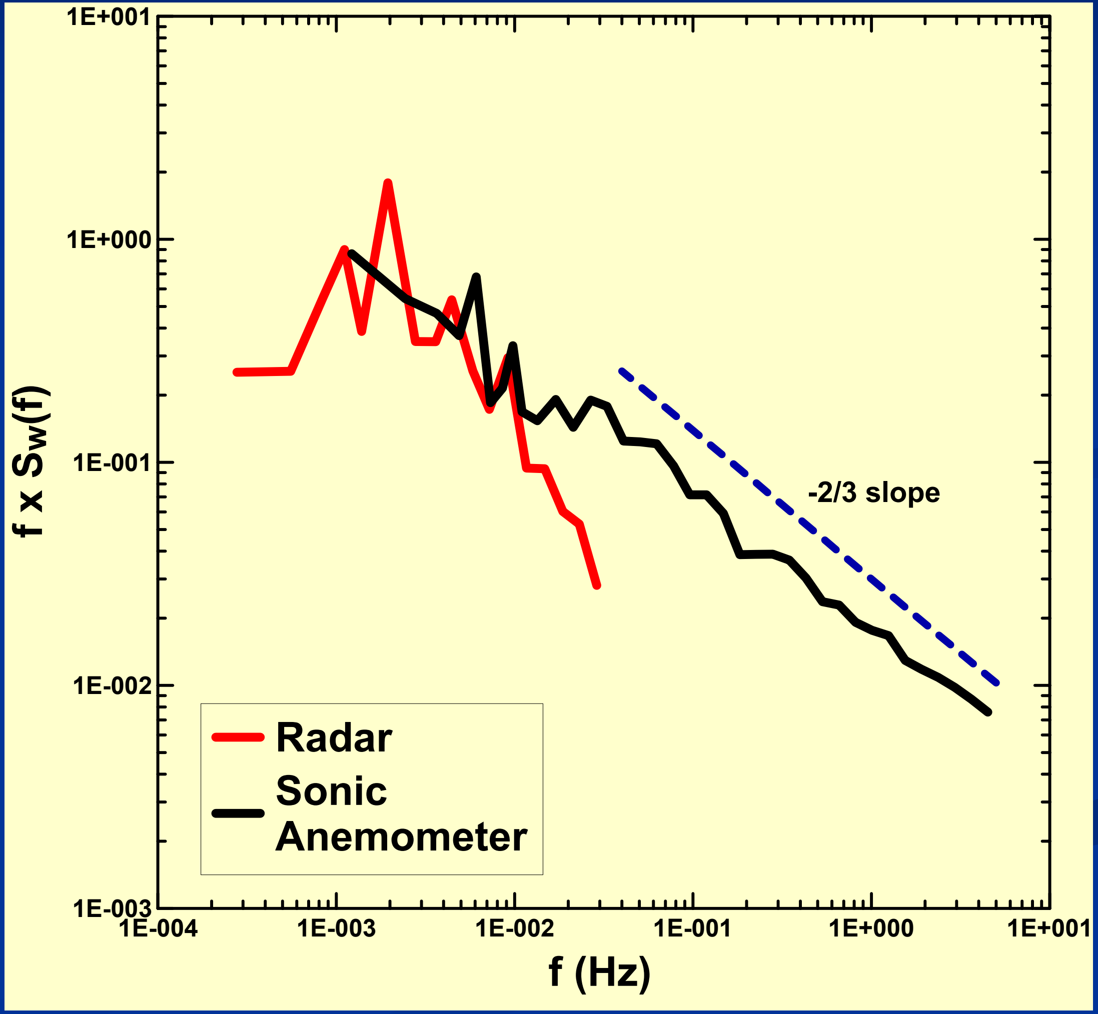

Estimating Turbulence Intensity

Beam broadening

Factors other than turbulence broaden the measured Doppler velocity spectrum. Because of the radar's finite beamwidth, a range of velocities are detected in the pulse volume, which broadens the spectrum. Empirical corrections have been developed to compensate for this and other effects.

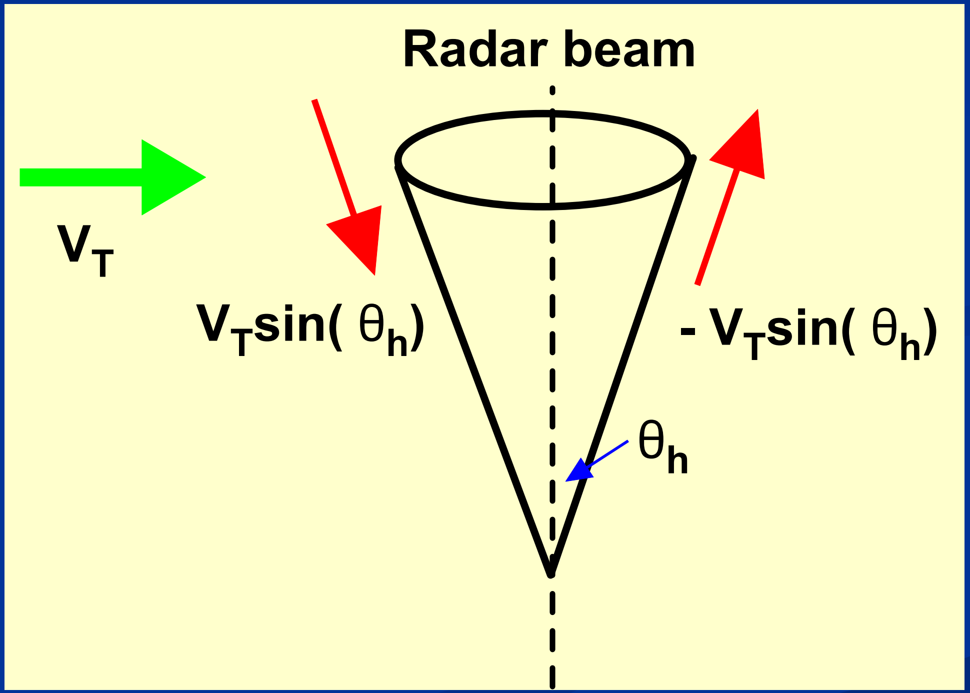

Estimating Turbulence Intensity

TKE dissipation rate

TKE dissipation rate

$$\sigma_{11}^{2} = \frac{\alpha \epsilon^{2/3}}{4\pi} \int\int_{-\infty}^{\infty}\int k^{-11/3} \left[1 - \left(\frac{k_1}{k}\right)^2\right] \left[1 - \underbrace{\frac{\sin^2(k_2 L/2)}{(k_2 L/2)^2}}_{\text{dwell filter}} \underbrace{\exp[-b^2 k_1^2 - a^2(k_2^2 + k_3^2)]}_{\text{pulse volume filter}}\right] dk_1\, dk_2\, dk_3$$

Radar spectral width adjusted for non-turbulent broadening

Note that the radar sampling filters are coupled and interact non-linearly in this equation. Unfortunately, full 3-D form requires numerical integration.

Estimating Turbulence Intensity

TKE dissipation rate

A double integral approximation has been developed which is accurate to within 2% of the full integral solution for all values of *L*. This approximate formula can be evaluated using readily available mathematical computation software. See White et al., 1999 for more details.

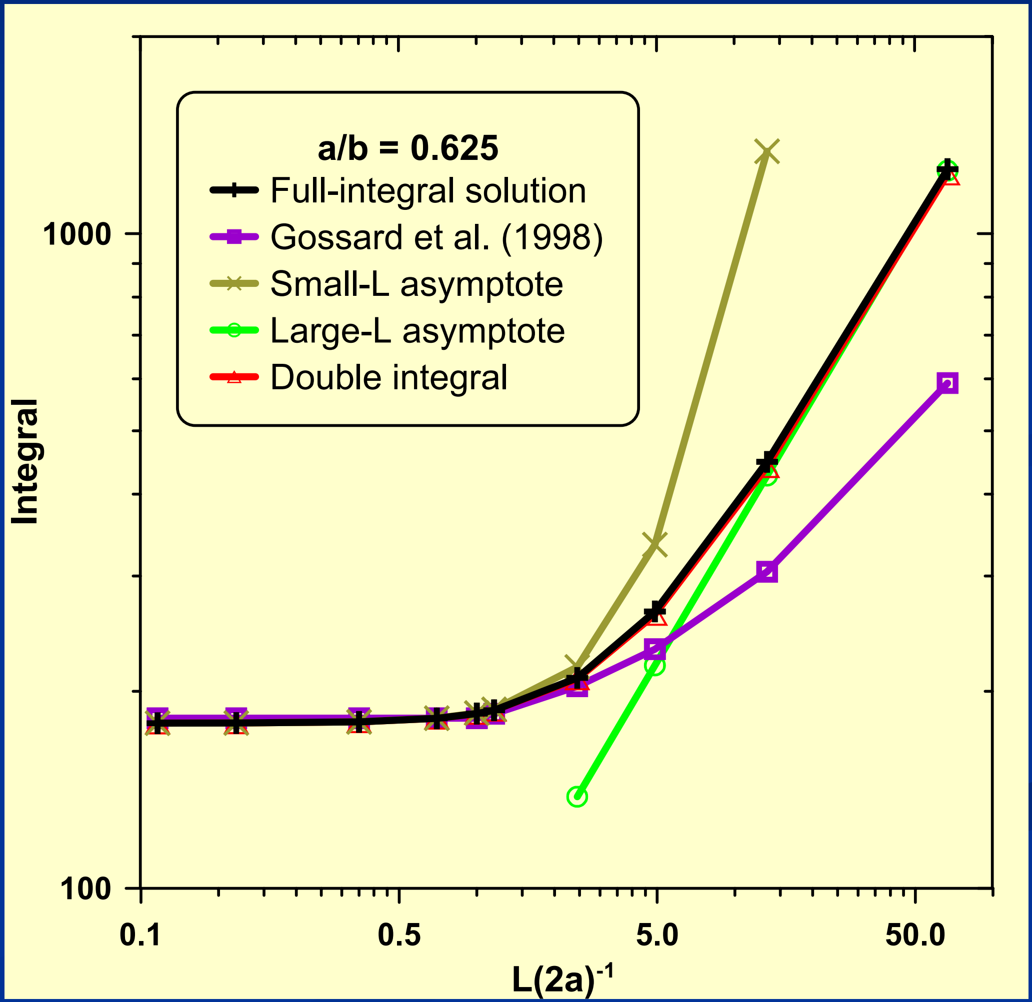

Estimating Turbulence Intensity

TKE dissipation rate

W.J. Shaw and J.M. Hubbe, 2000 AMS Conf. on Mountain Meteorology

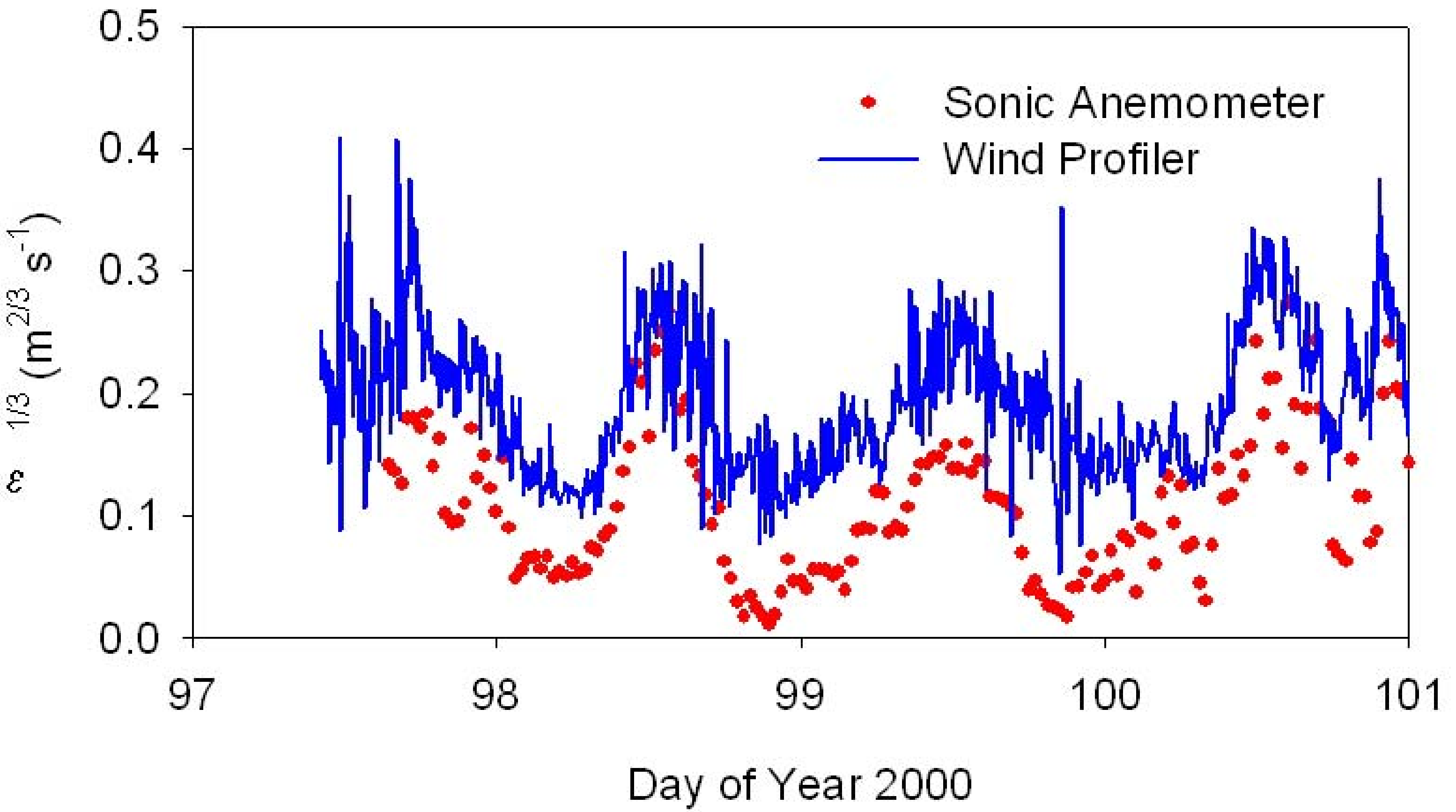

Sodar Backscatter Echoes

Boundary-layer height

In the atmosphere, sound scatters from fluctuations in temperature and, to a lesser extent, humidity and velocity. Neglecting velocity and humidity contributions, the acoustic scattering cross-section is proportional to the temperature structure function parameter, C_T^2, of turbulence theory, which exhibits a peak at the boundary-layer capping inversion.

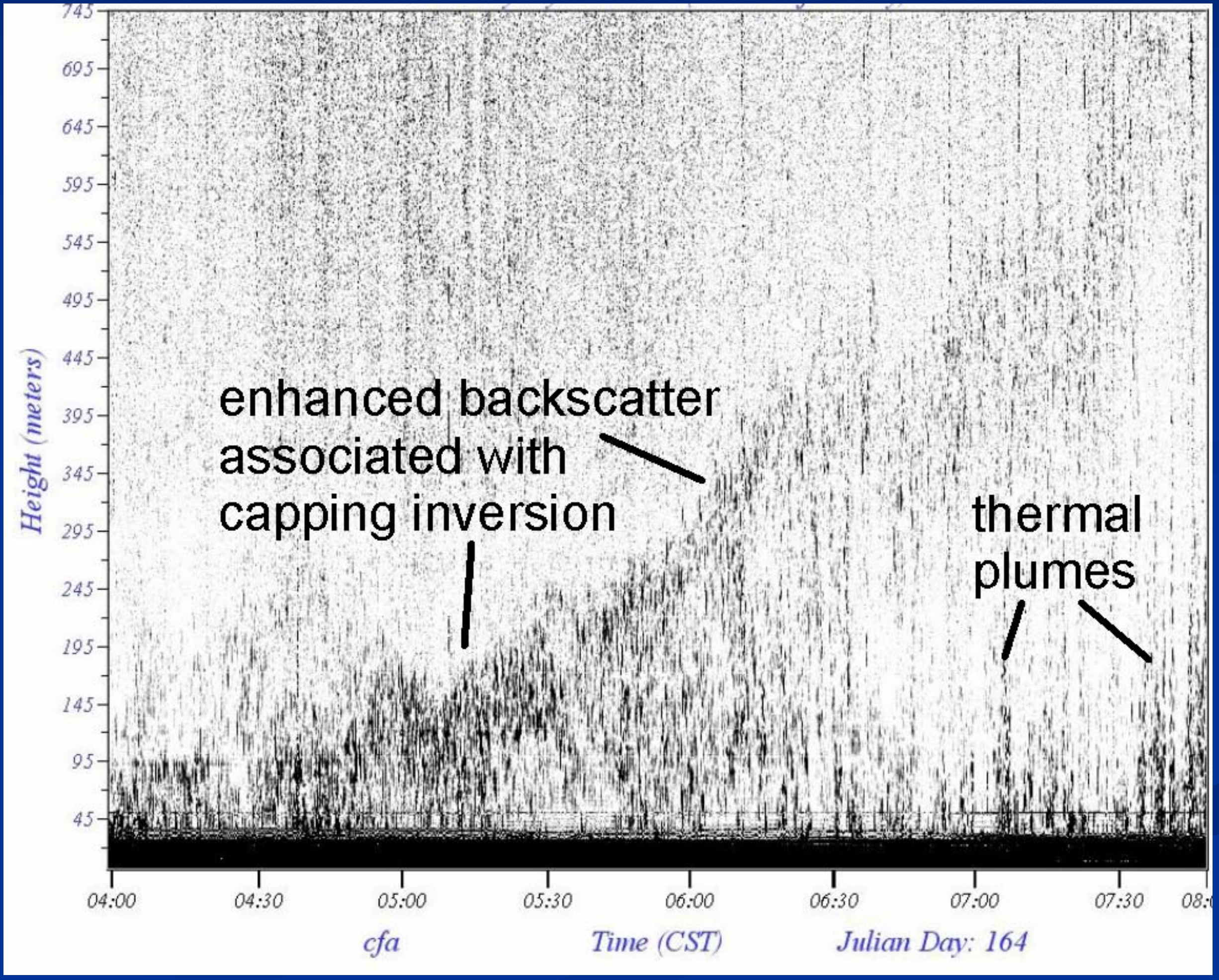

Sodar Backscatter Echoes

Thunderstorm gust front

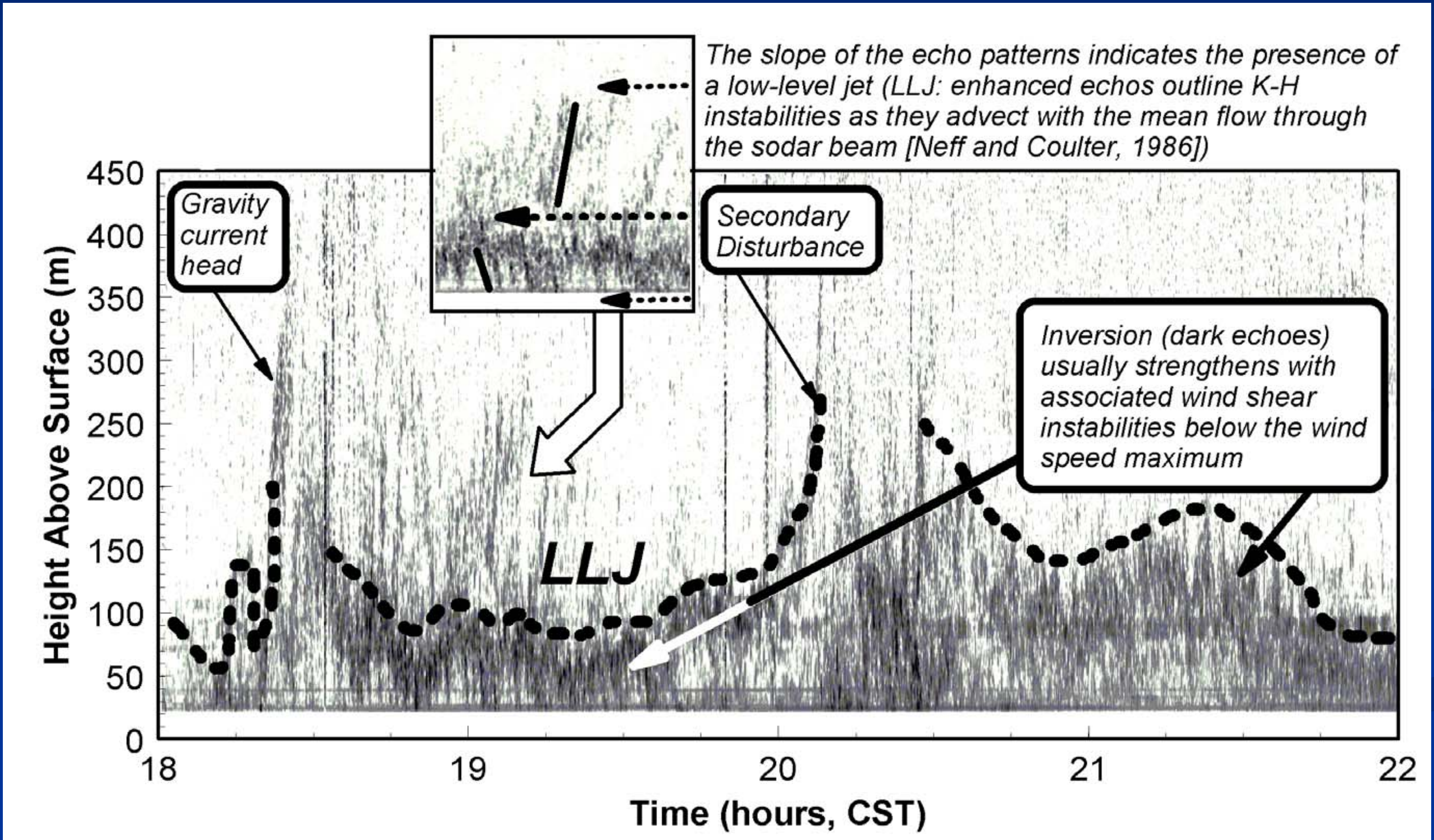

Fronts

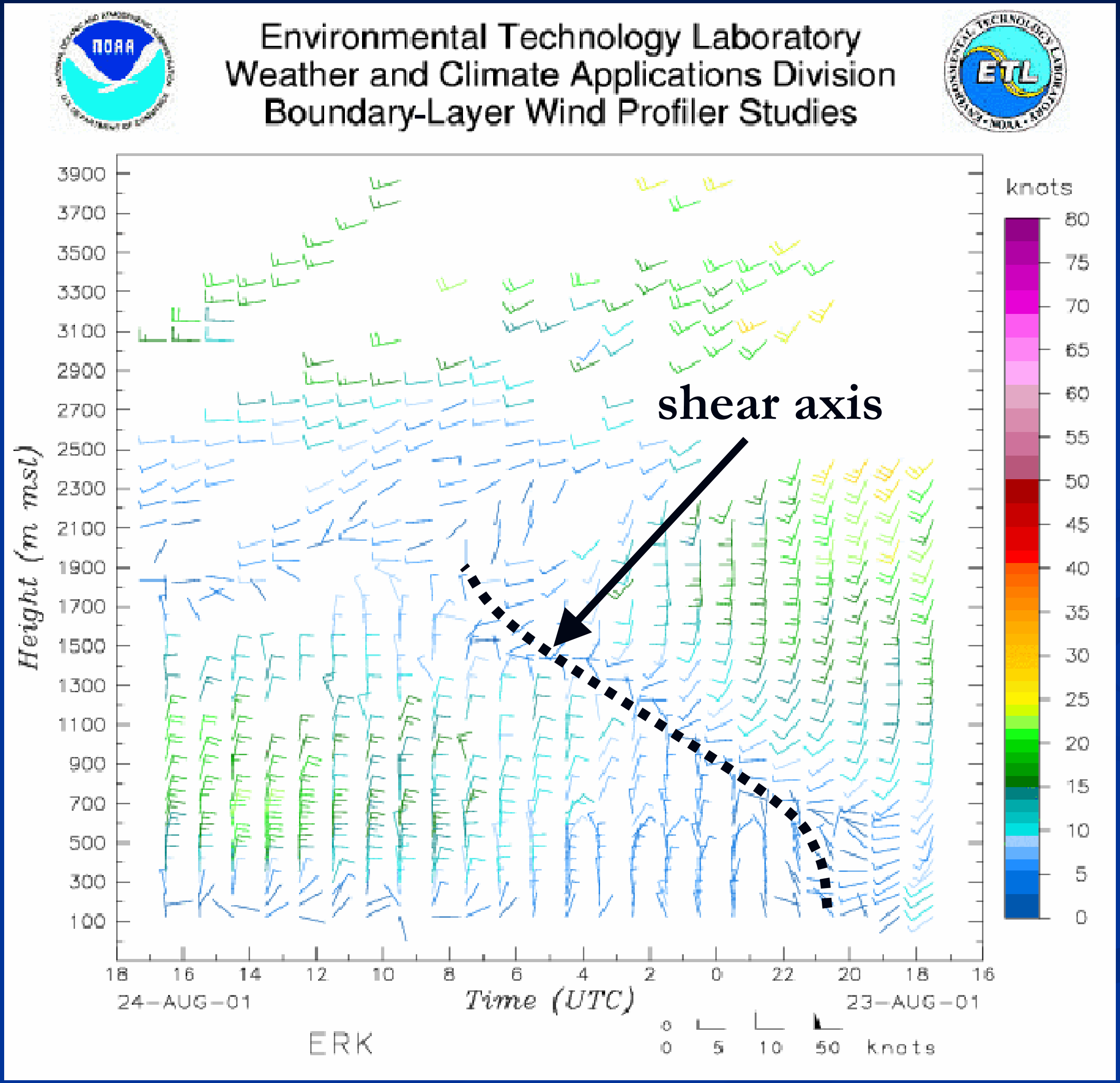

Environmental Technology Laboratory
Weather and Climate Applications Division
Boundary-Layer Wind Profiler Studies
shear axis
Height (m msl)
3900
3700
3500
3300
3100
2900
2700
2500
2300
2100
1900
1700
1500
1300
1100
900
700
500
300
100
knots
80
75
70
65
60
55
50
45
40
35
30
25
20
15
10
5
0
18 16 14 12 10 8 6 4 2 0 22 20 18 16
24-AUG-01
Time (UTC)
23-AUG-01
ERK
0 5 10 50 knots

Fronts

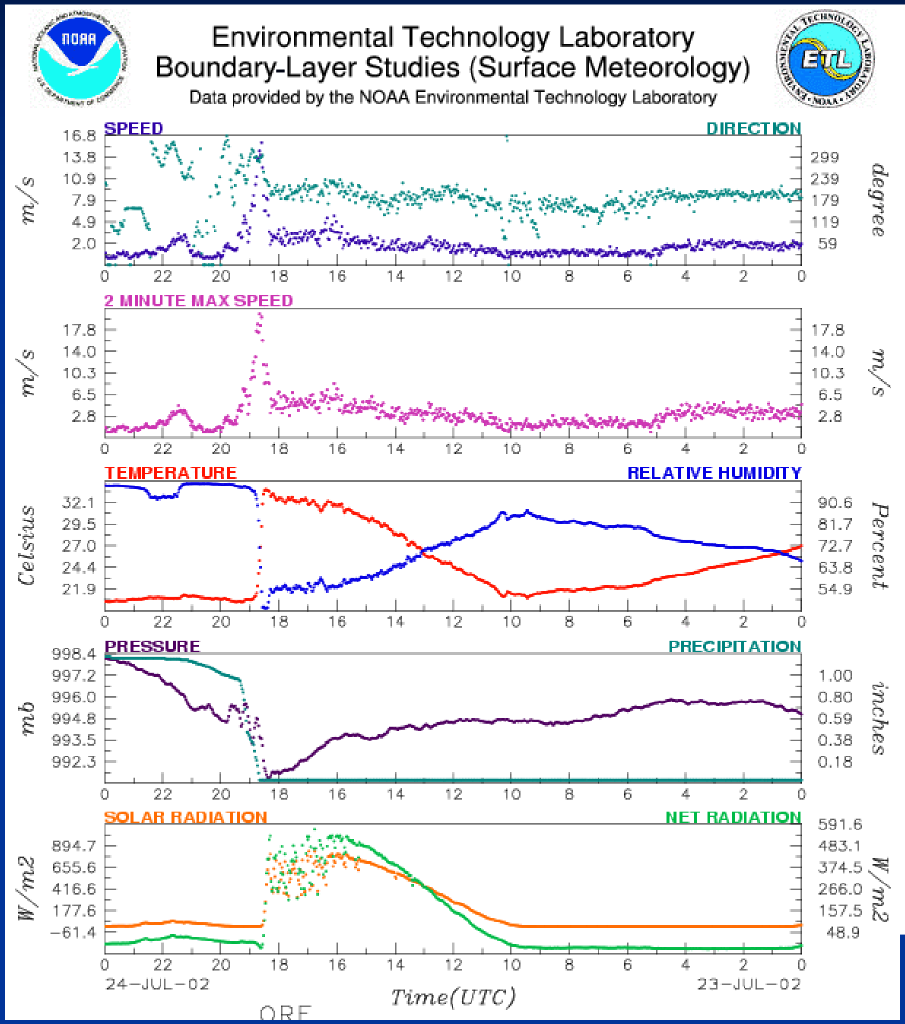

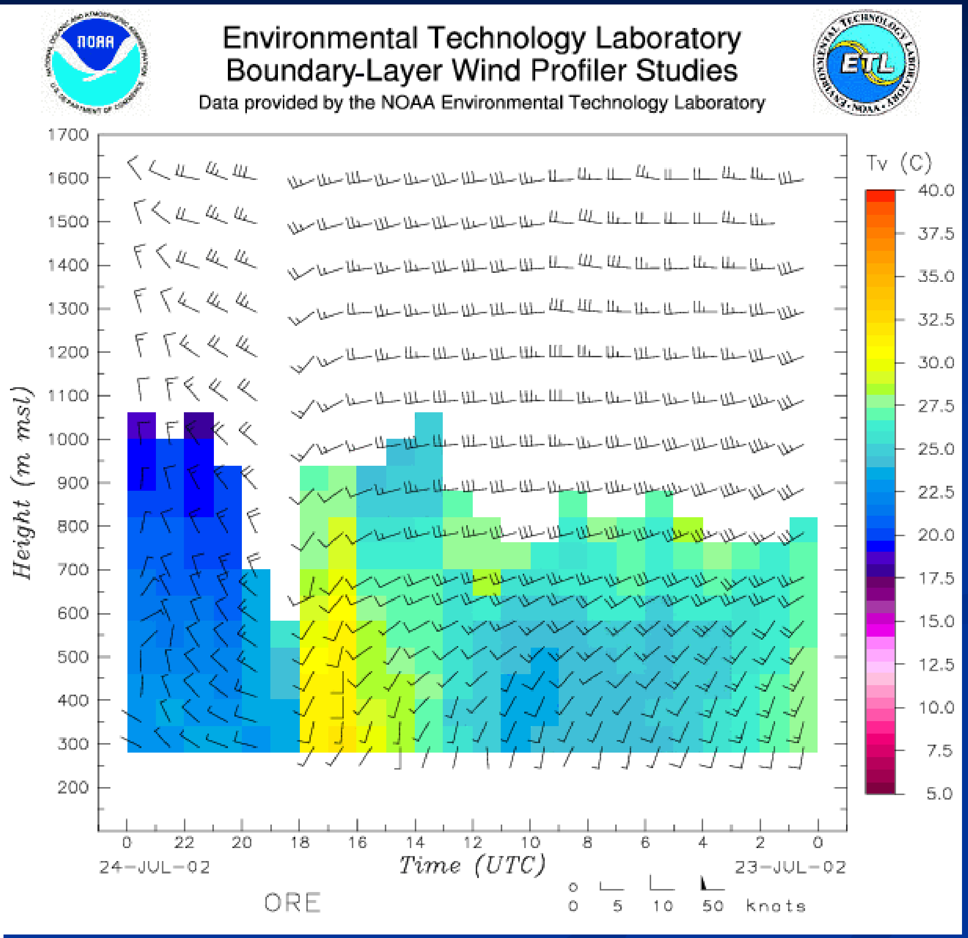

RASS virtual temperature

Surface meteorology

Fronts

Descending warm front: contours of zonal wind speed

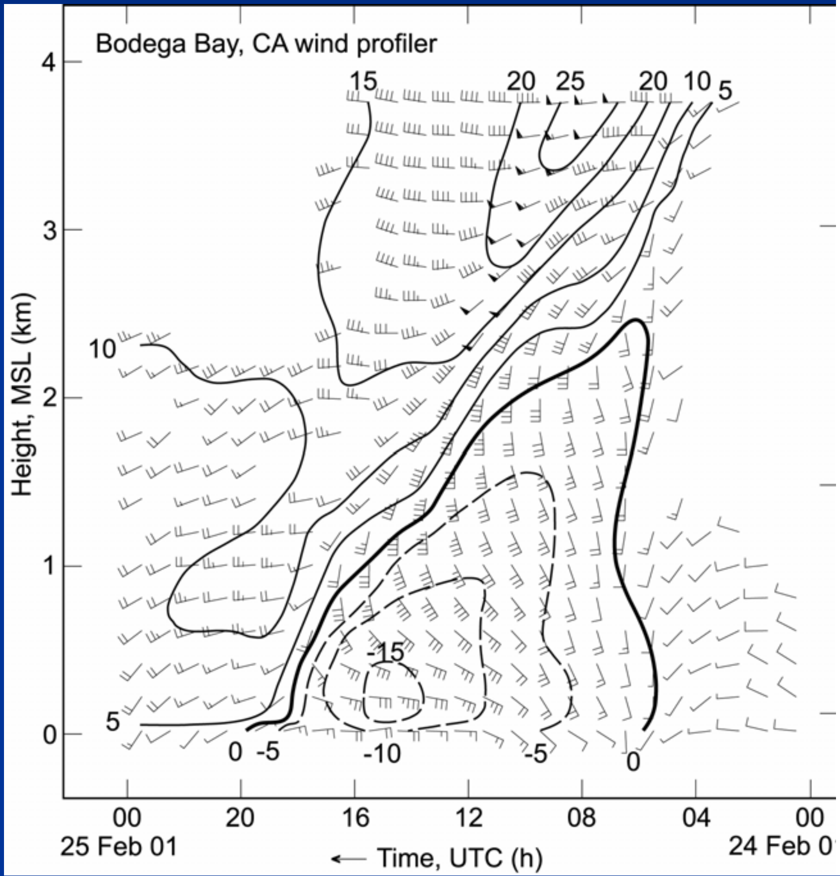

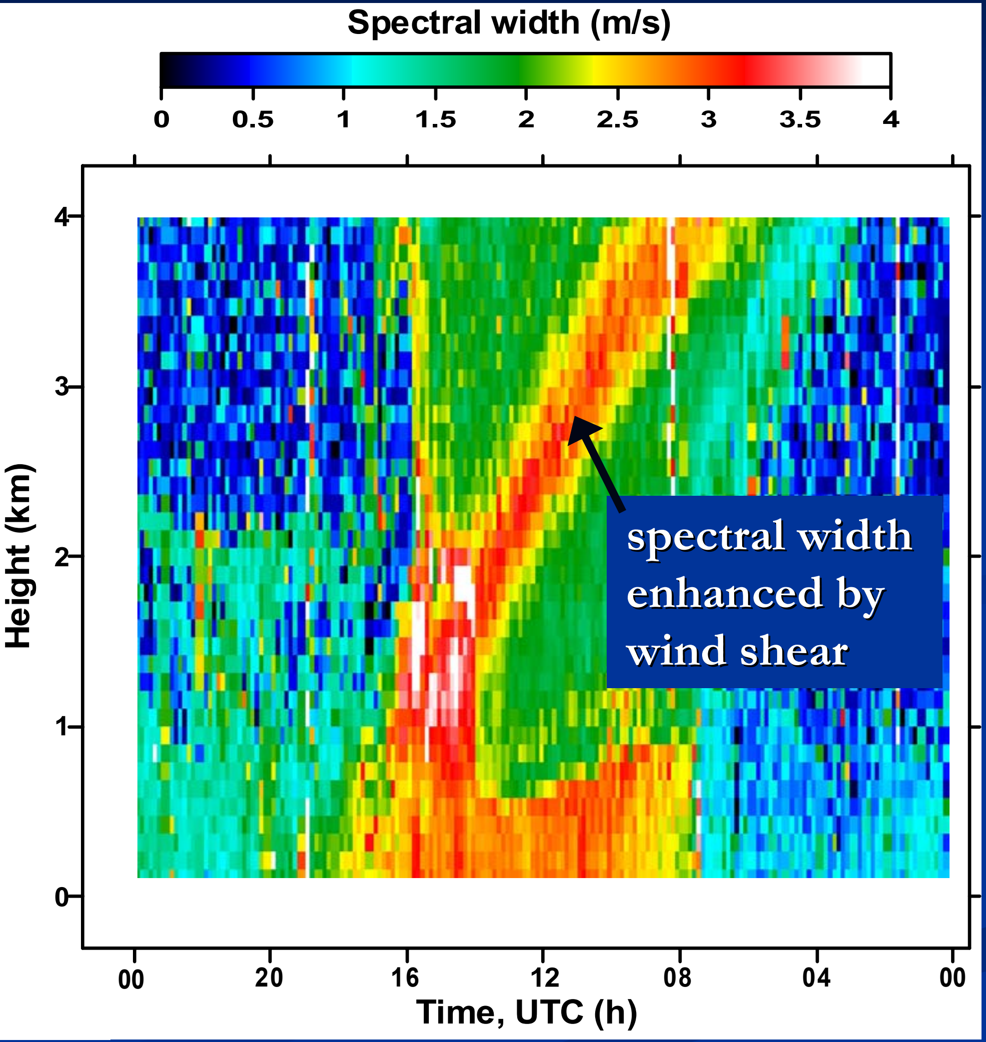

Low-level Jets

Monthly diurnally averaged winds from a site near Tampa Bay, Florida, indicating the mean timing of a nocturnal low-level jet exceeding 10 m s^{-1}. This type of jet occurs under weak synoptic forcing and at night as the effects of surface friction are decoupled from the winds aloft.

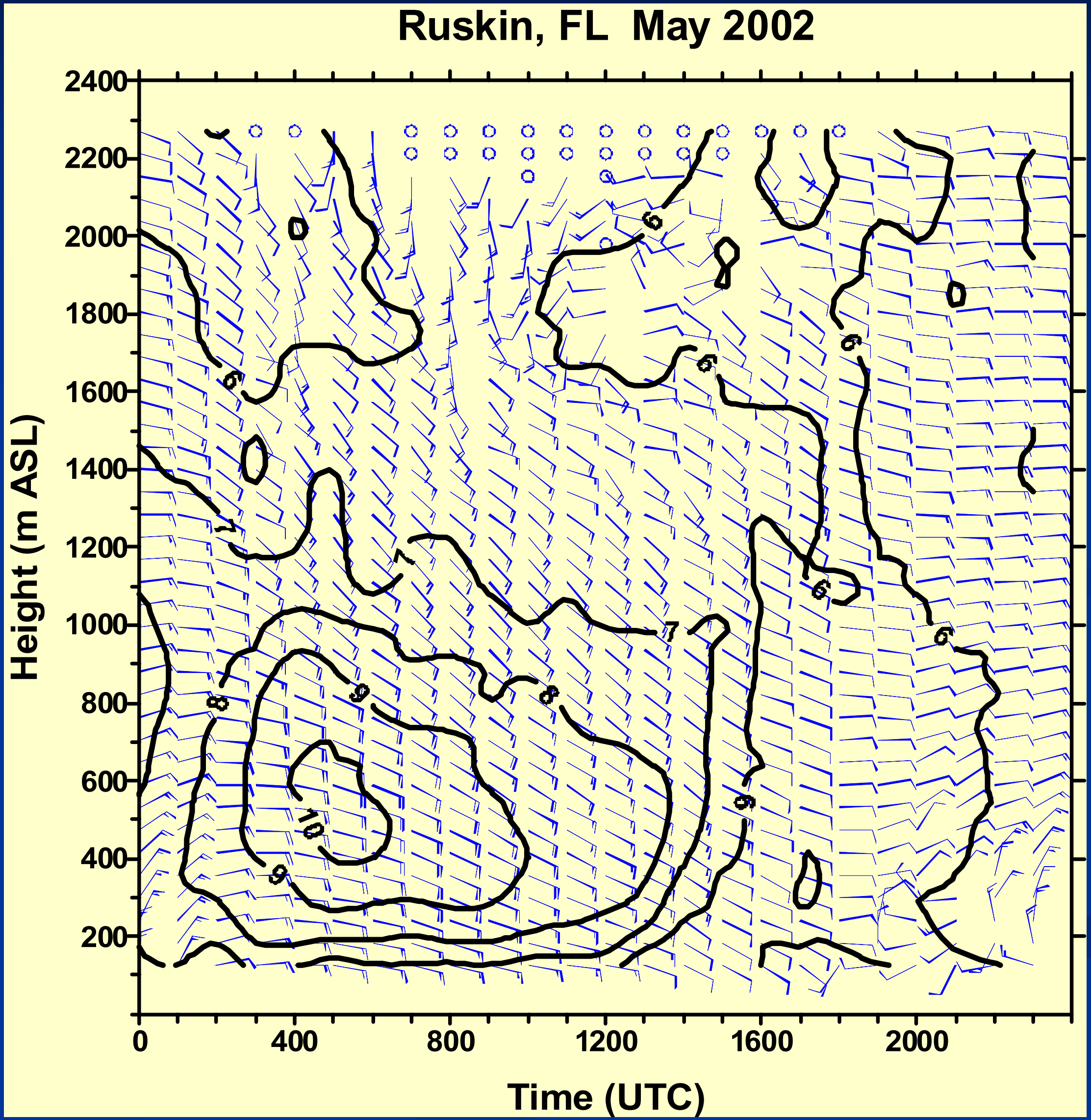

Low-level Jets

Forward trajectories derived from a network of wind profilers deployed in and around Nashville, Tennessee, show the combined effects of the nocturnal low-level jet and the inertial oscillation. Both effects contribute to varying with altitude the transport of pollutants.

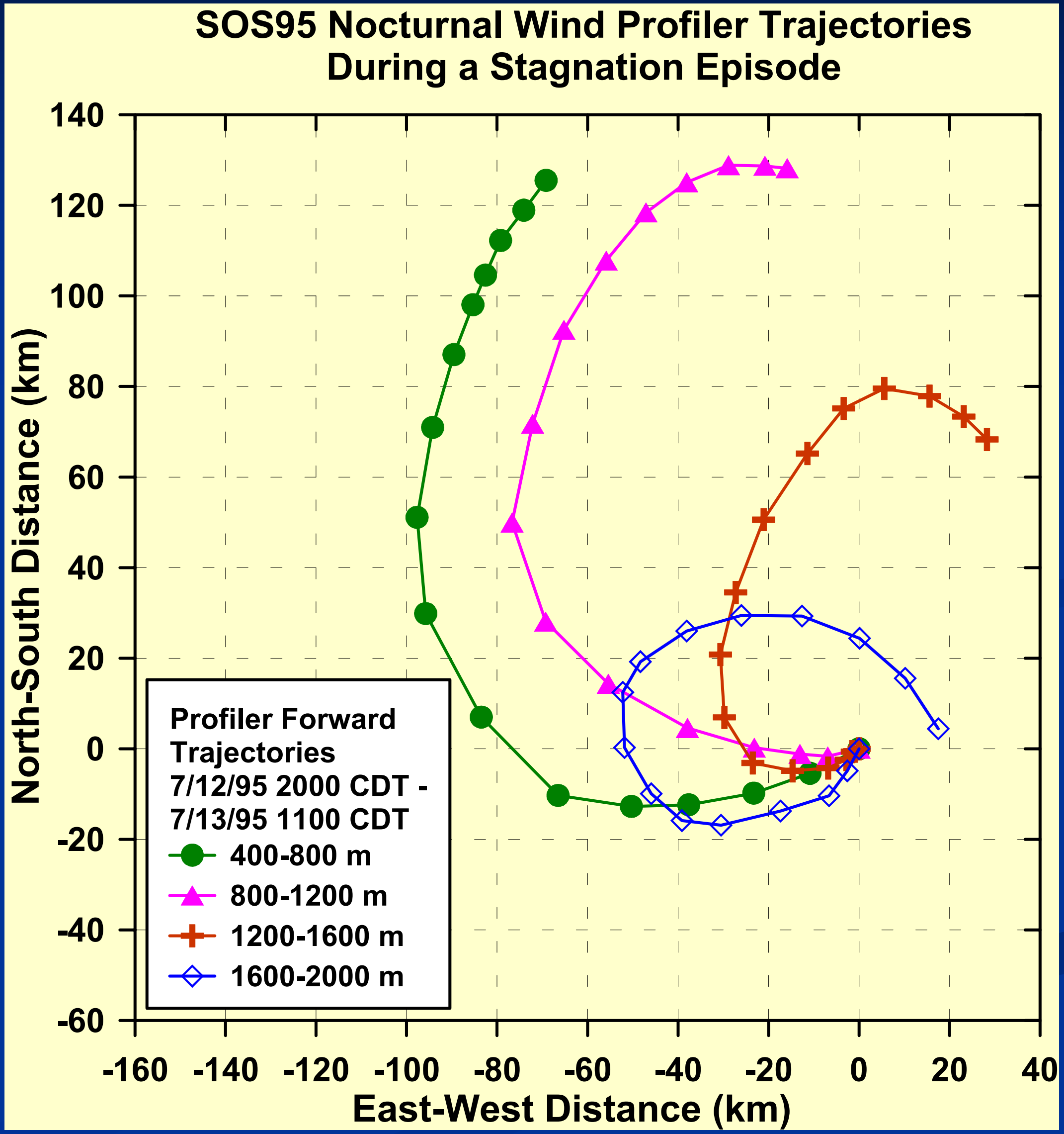

Low-level Jets

Orographic rains on the windward side of coastal mountains are enhanced when a low-level jet increases the flow of moisture-laden air onshore. In this case the offshore measurements were provided by the NOAA P-3 Orion research aircraft flying offshore of California during CALJET. The correlation profile was produced using coastal wind profiler observations. This type of jet is baroclinically and frontally forced.

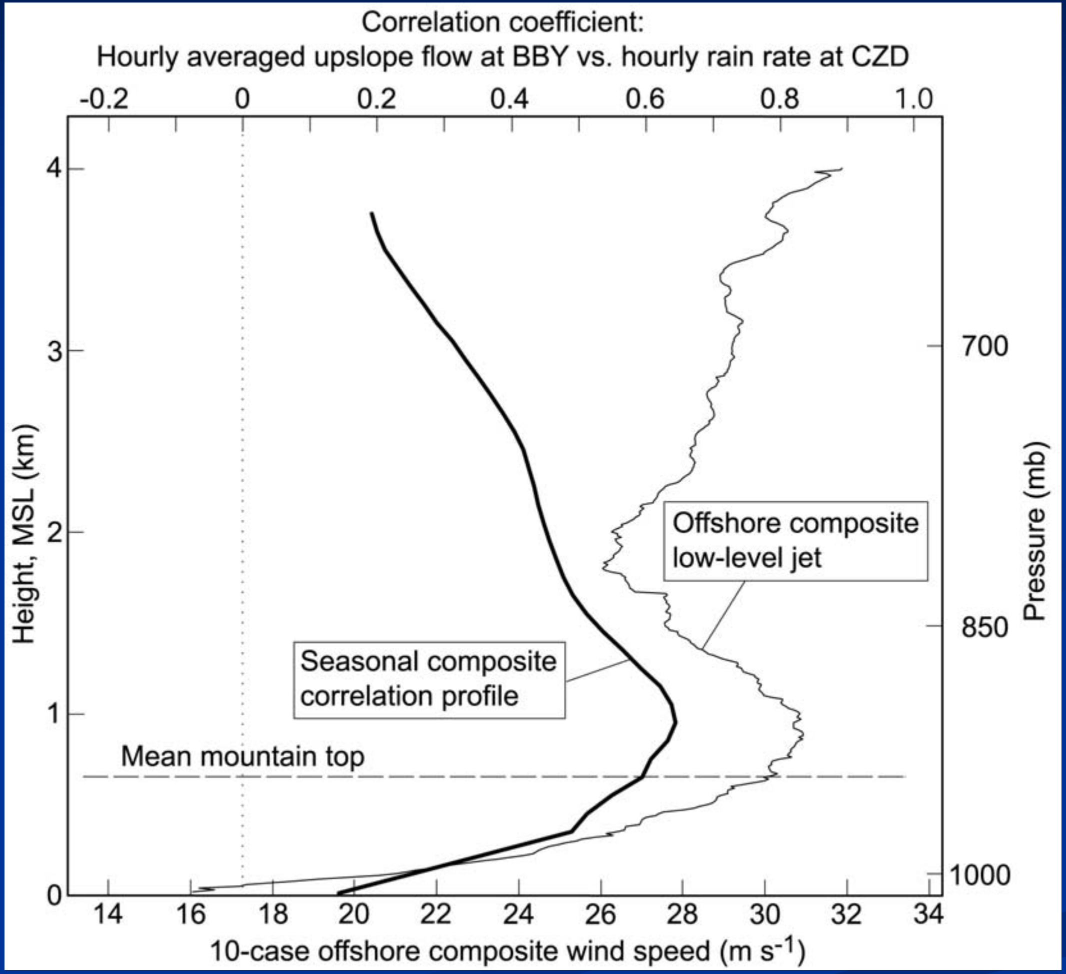

See Neiman et al., *Mon. Wea. Rev.*, 2002

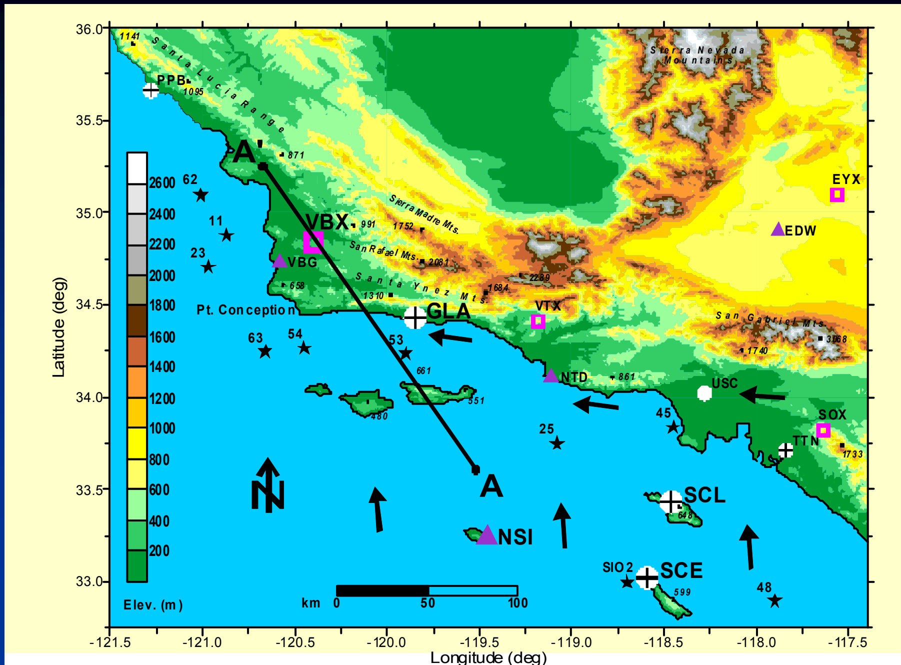

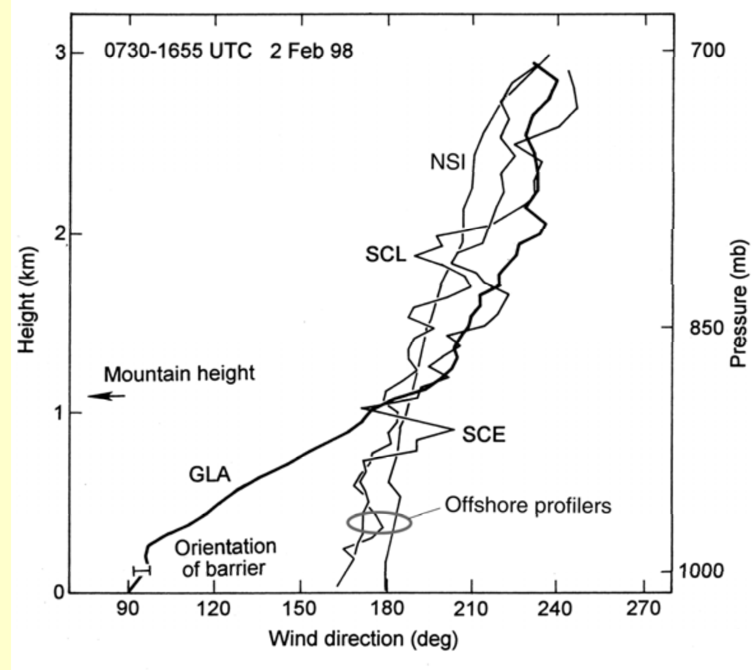

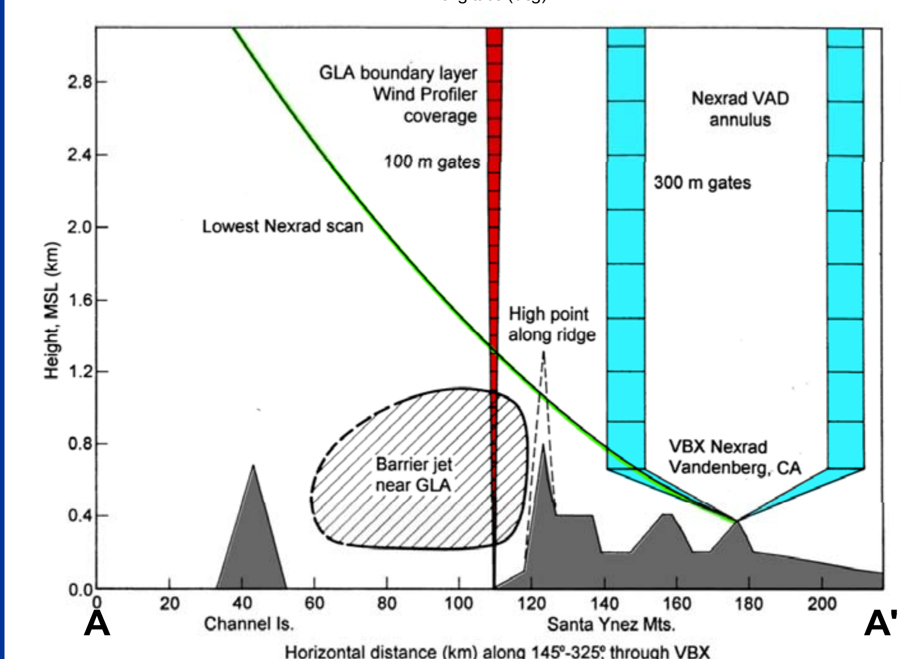

- **Coastal and island wind profilers used in CALJET documented blocked flow along the Santa Barbara coast.**
- **The nearest NEXRAD radars miss this blocked flow, both in the lowest scan and in VAD wind profiles, because of their respective locations and altitutdes.**
- **Wind profiler data were made avaiable to NWS forecasters in real time, filling an important data gap in the current observing system.**

Profiler Precipitation Measurements

- Signatures of precipitation are reflected in all three Doppler spectral moments (velocity, reflectivity, spectral width).
- For the 915 MHz BLPs, the primary scattering mechanisms are Bragg (clear air) and Rayleigh (precipitation). In rain, the Rayleigh component usually dominates.
- In precipitation, the reflectivity measured by the radar is an integrated measurement over all drop sizes measured within in the scattering volume. Larger drops dominate because reflectivity is diameter-to-the-sixth-power dependent.
- The Doppler velocity measured by the radar is reflectivity weighted, i.e., again, the larger drops dominate.
- For accurate wind profiling in precipitation, it is necessary to remove the Doppler vertical velocity from the oblique beams.

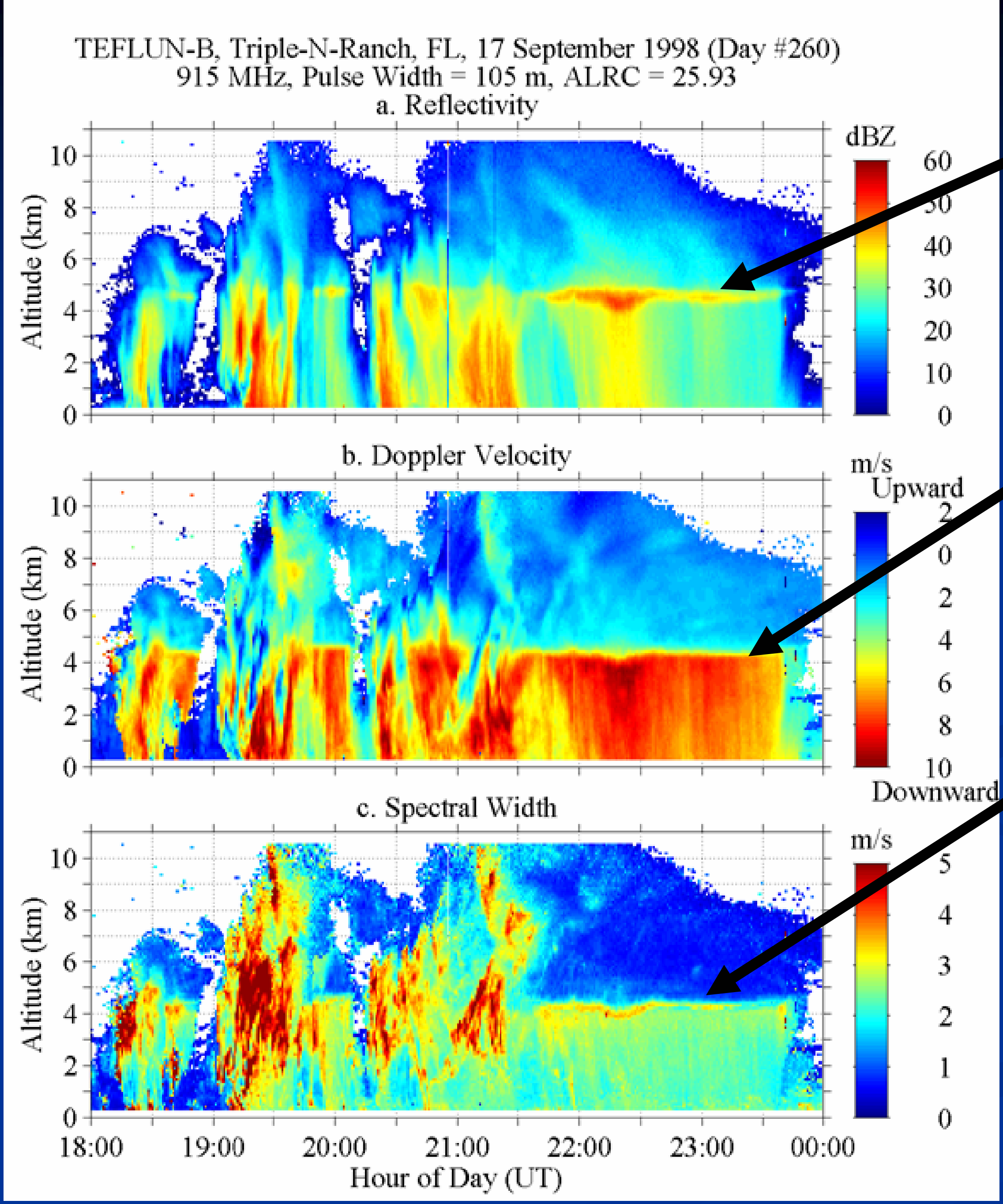

Stratiform Rain

Brightband

Enhancement in reflectivity due to water coating of ice particles.

Doppler Velocity Gradient

Difference in fallspeed between ice and water.

Increase in Spectral Width

Fallspeed distributions are narrower for ice than for water.

Courtesy of Chris Williams, CIRES, NOAA/AL

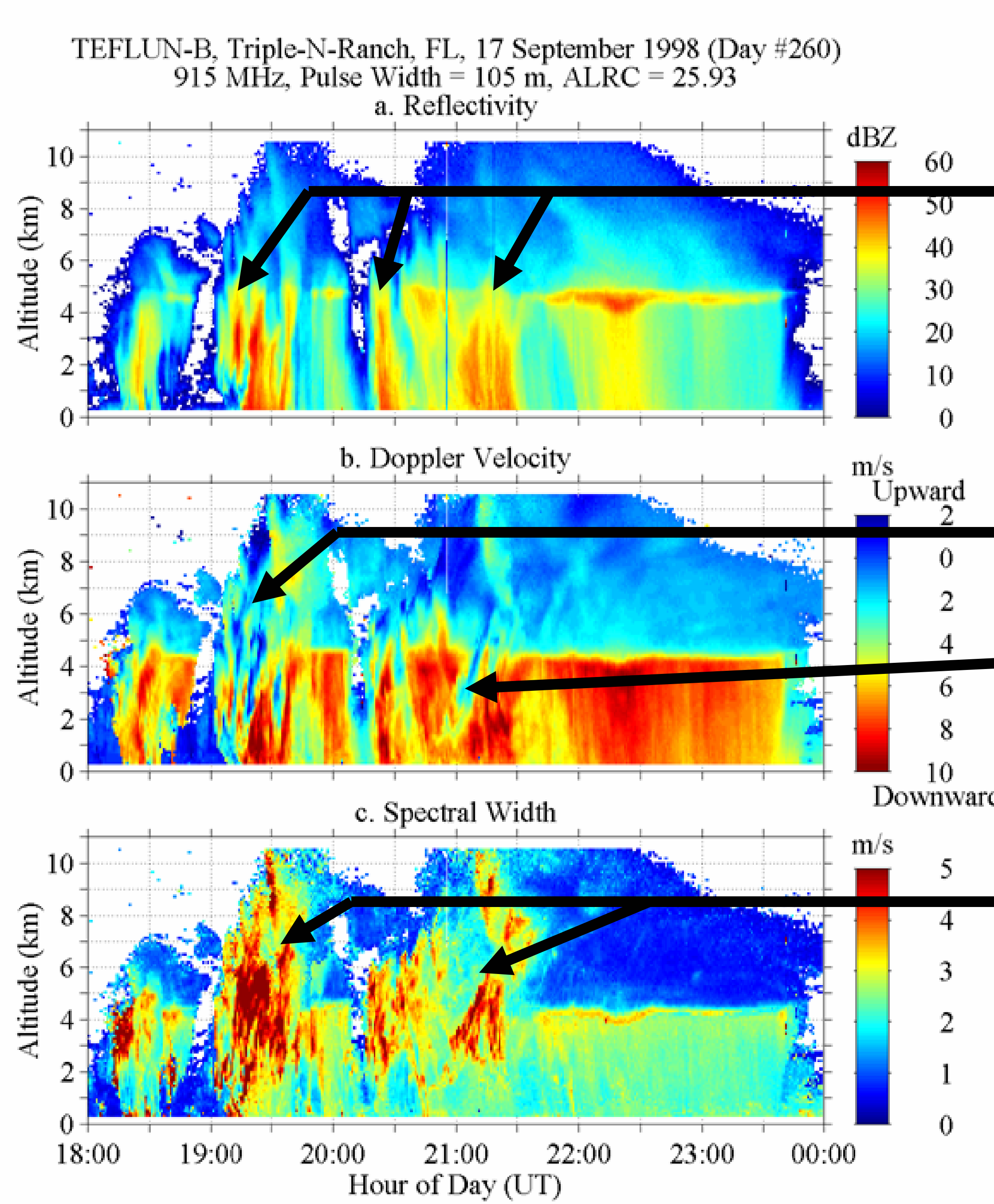

Convective Rain

Vertical Structure of Reflectivity

No Brightband

Variations in Doppler Velocity

Possible net upward motion

Enhanced Spectral Width

Indicating increased turbulence

Courtesy of Chris Williams, CIRES, NOAA/AL

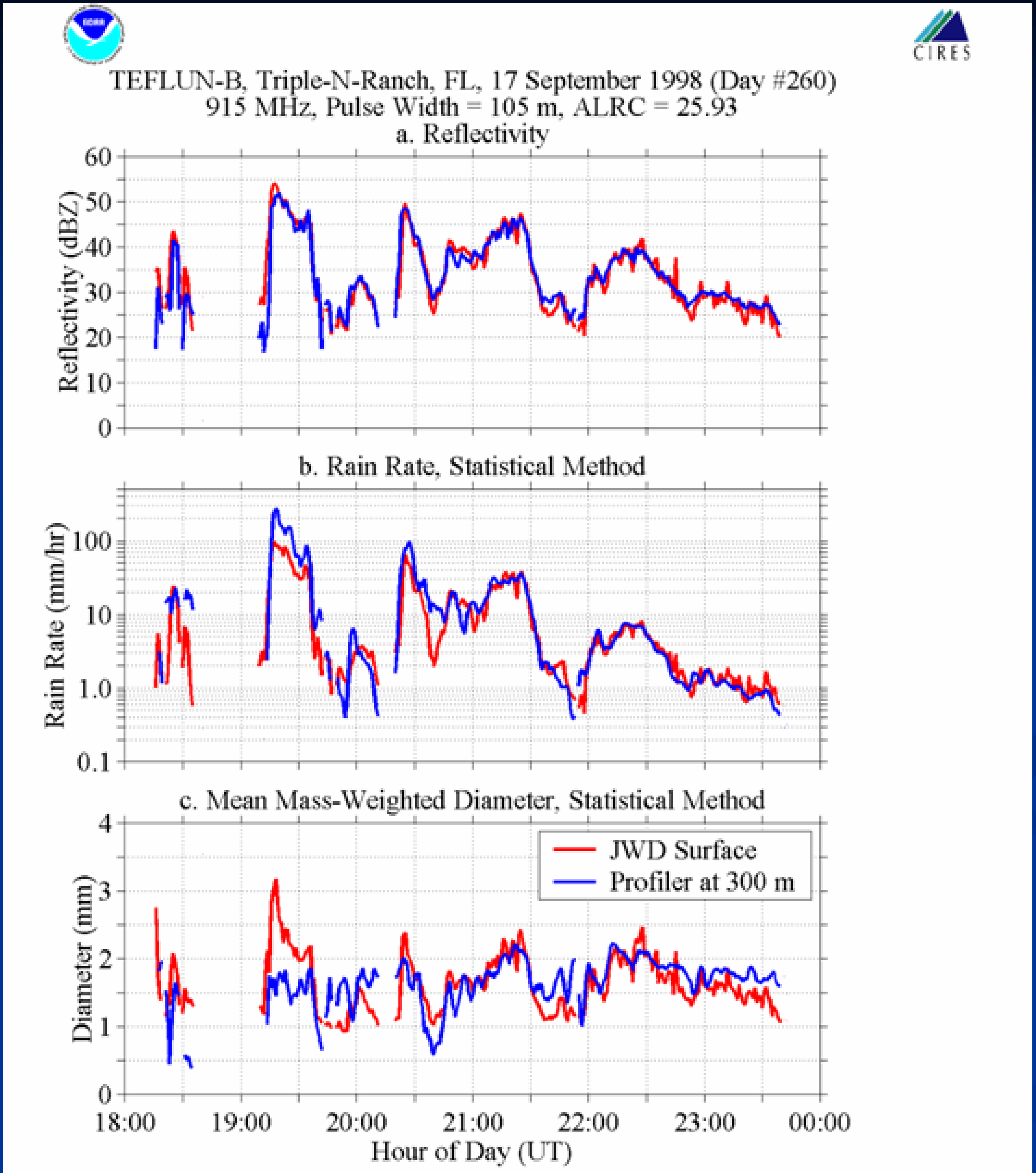

Microphysical Retrievals

Comparison of profiler retrieved values at 300 meters with surface disdrometer observations.

Top: Reflecitivity

Middle: Rain Rate

Bottom: Mean Mass Weighted Diameter, D_m

Williams, Radio Sci., 2002

Calculating Winds in Precipitation

No vertical correction applied

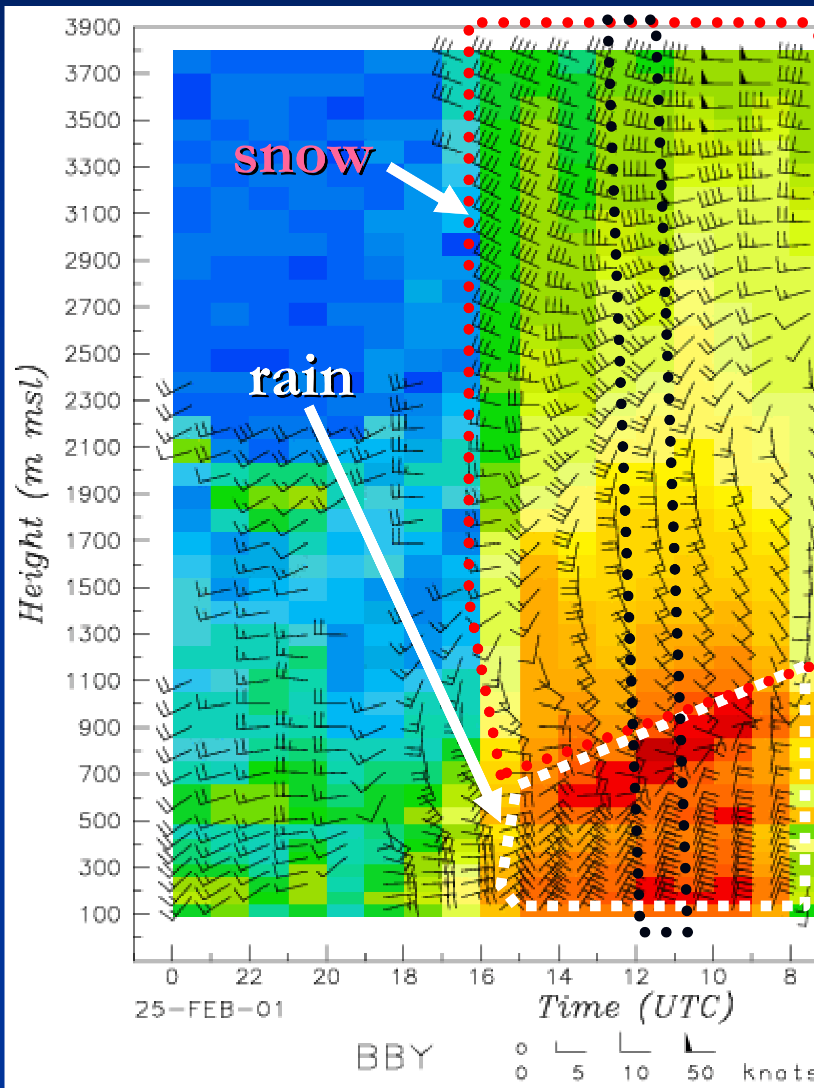

Vertical correction applied

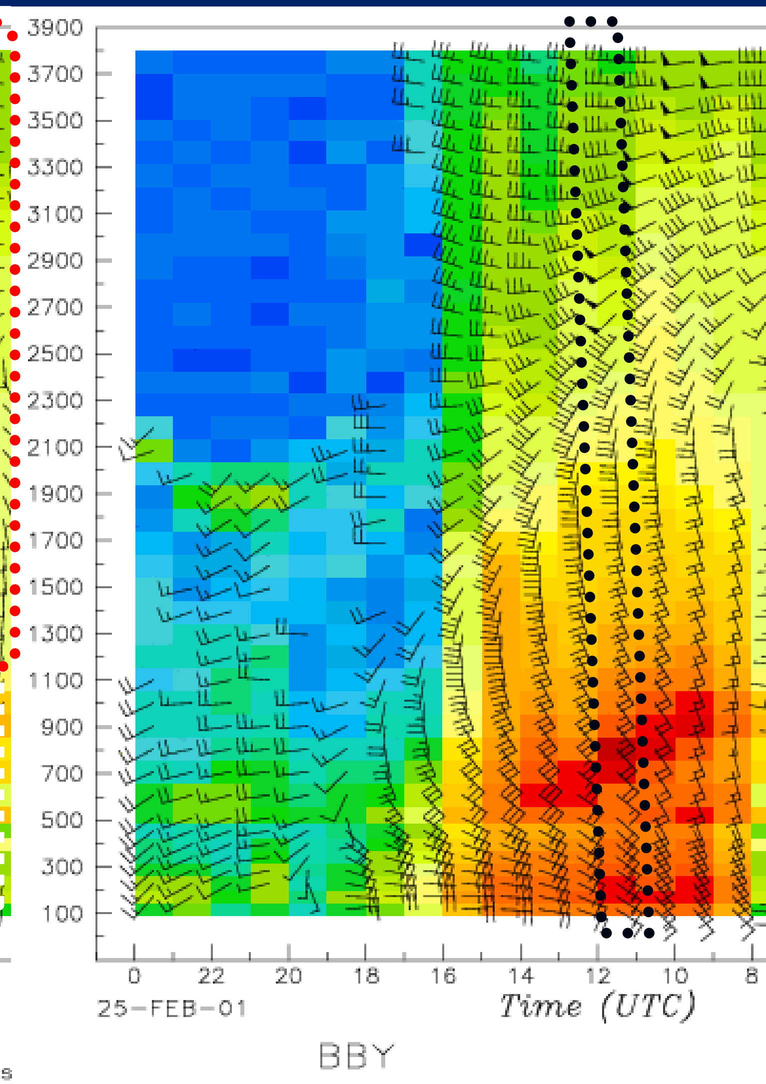

N S V

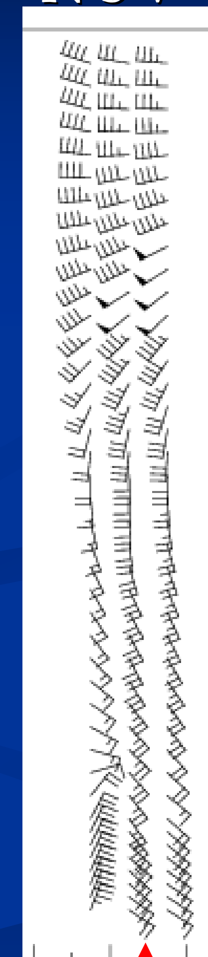

Sounding at 11:26 UTC

Profiler Snow-level Algorithm

- Takes advantage of the fact the wind profilers measure Doppler vertical velocity in order to compute the three-dimensional wind vector, whereas many scanning precipitation radars do not adopt this strategy.

- The bright-band height is a better estimate of the snow level than the melting level (i.e. 0o C isotherm) because of the time (or fall distance) required for ice particles to melt as they descend.

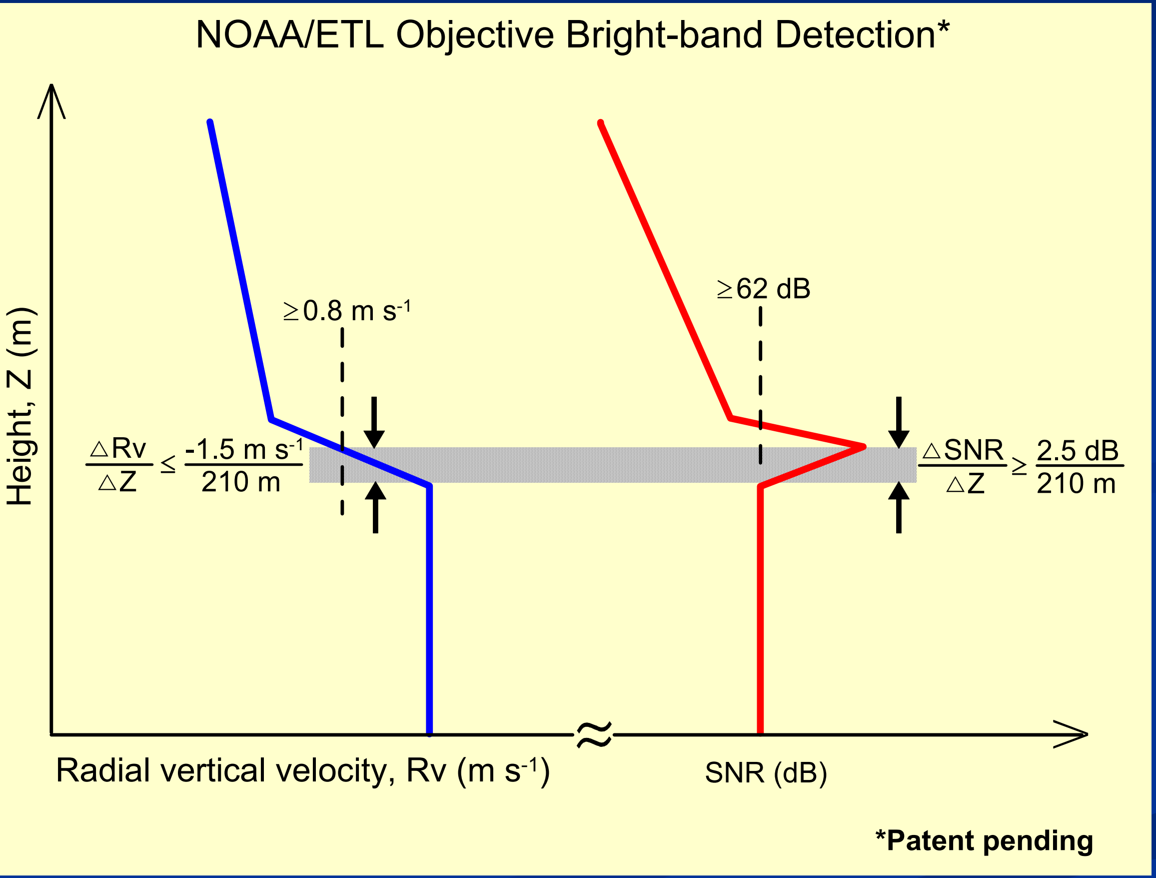

White et al., 2002 (JTech)

Profiler Snow-level Algorithm

Background field of consensus Doppler vertical velocity (Rv, positive downward) showing the transition from snow to rain. The snow-level estimates from the algorithm are indicated by the black dots. The table, which was added at the request of NWS weather forecasters, lists the snow level along with the surface temperature measured by a met station collocated with the wind profiler.

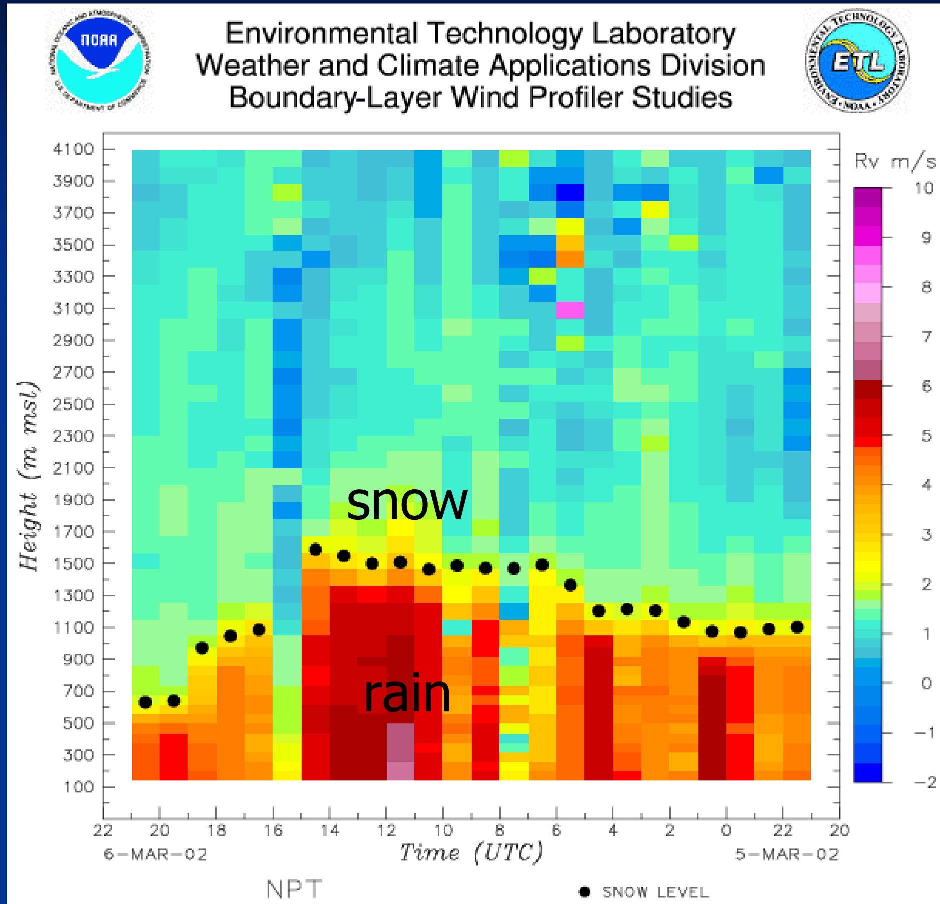

Time (UTC)	2030	1930	1830	1730	1630	1530	1430	1330	1230	1130	1030	0930
Snow Level (m)	631	640	971	1046	1086	none	1588	1548	1500	1508	1464	1487
Snow Level (ft)	2069	2099	3184	3430	3562	none	5208	5077	4919	4946	4801	4877
Sfc Temp (C)	6.02	6.18	6.24	5.97	6.31	6.87	7.23	7.43	9.44	9.92	10.04	10.14

Time (UTC)	0830	0730	0630	0530	0430	0330	0230	0130	0030	2330	2230	2130
Snow Level (m)	1471	1469	1492	1365	1204	1215	1206	1134	1075	1069	1090	1102
Snow Level (ft)	4824	4818	4893	4477	3949	3985	3955	3719	3525	3506	3575	3614
Sfc Temp (C)	10.02	7.28	7.25	7.36	7.31	7.30	7.80	8.41	8.55	8.13	8.72	9.06

Profiler Snow-level Algorithm

Snow-level image generated during a November 2002 ice storm that affected millions in the Northeast. The data shown here were collected at Concord, New Hampshire, on November 17. Note the relatively high snow level with sub-freezing temperatures occurring at the surface.

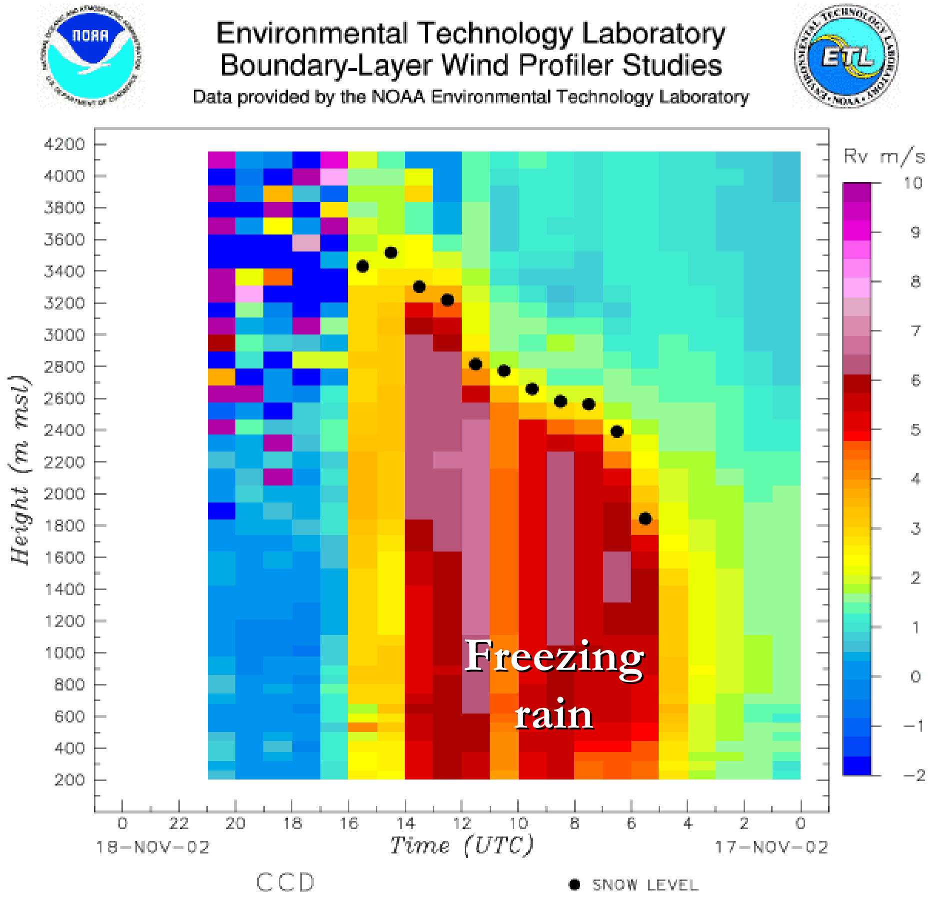

Time (UTC)	2330	2230	2130	2030	1930	1830	1730	1630	1530	1430	1330	1230
Snow Level (m)					none	none	none	none	3431	3517	3302	3219
Snow Level (ft)					none	none	none	none	11253	11535	10830	10558
Sfc Temp (C)					0.83	1.02	0.91	0.25	−0.01	−0.20	0.06	0.04

Time (UTC)	1130	1030	0930	0830	0730	0630	0530	0430	0330	0230	0130	0030
Snow Level (m)	2815	2773	2659	2581	2564	2392	1843	none	none	none	none	none
Snow Level (ft)	9233	9095	8721	8465	8409	7845	6045	none	none	none	none	none
Sfc Temp (C)	−0.11	−0.69	−1.91	−2.71	−2.91	−3.10	−3.19	−3.79	−4.07	−4.17	−3.94	−3.46

Profiler Snow-level Applications

River forecasting

- The two most important factors influencing runoff forecasts for mountainous watersheds are the quantitative precipitation forecast and the melting level.
- The model-based results shown to the right indicate that a 2000-ft increase in the melting level could triple the runoff in a watershed.

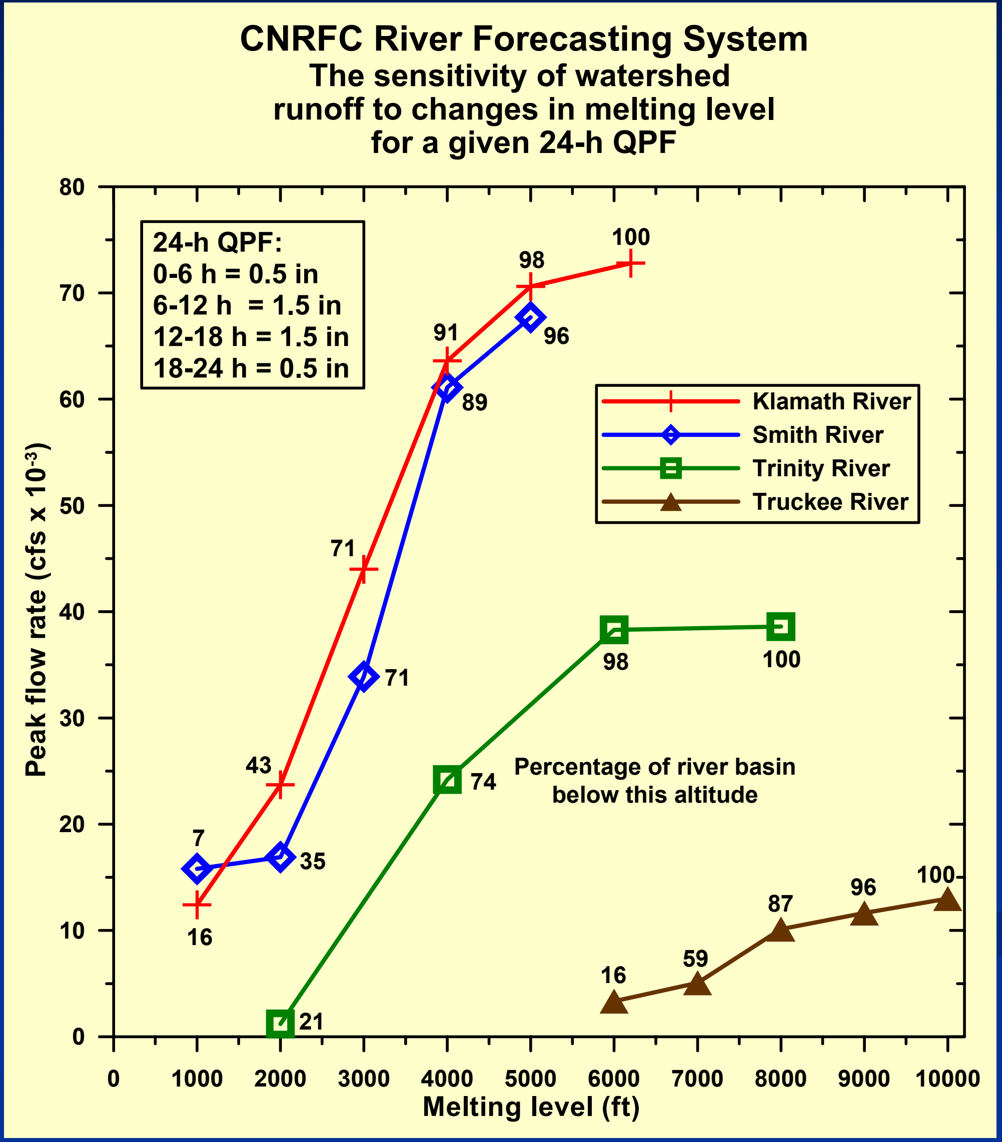

Profiler Snow-level Applications

Highway maintenance

- 6,600 fatalities per year in adverse weather
- 544 million hours ($2 billion) lost productivity

Source: U.S. Dept. of Transportation

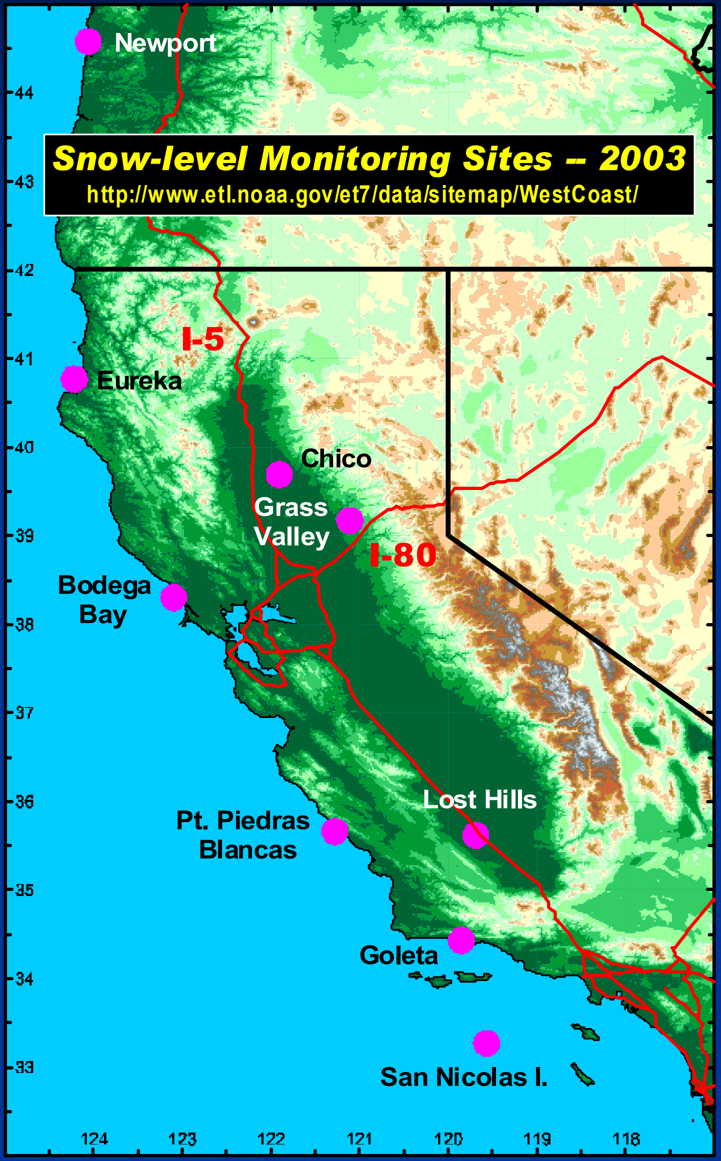

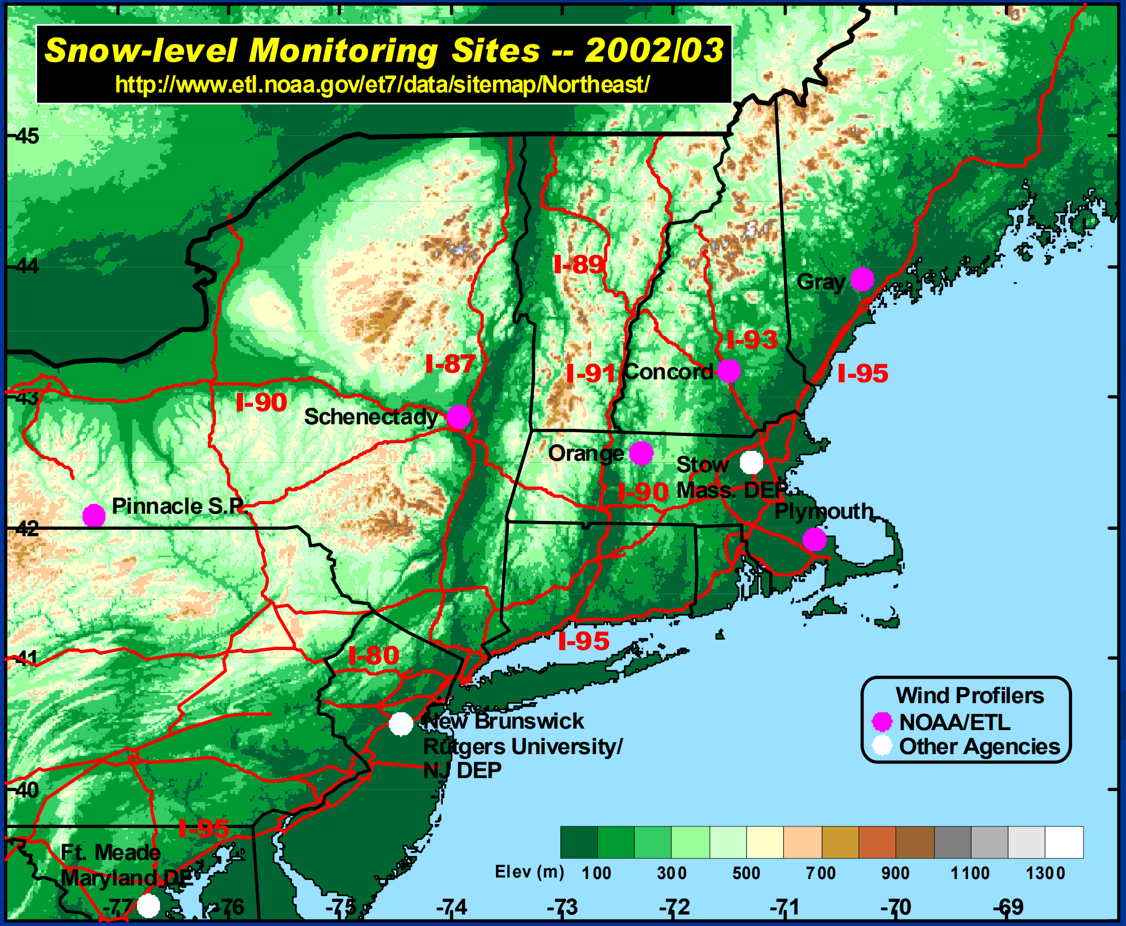

Operational Forecasting

Snow Advisory raised to Winter Storm Warning

- Prototype profiler snow-level product from PACJET showed 2700-ft snow level at the coast, 1300 ft lower than the snow level that had been predicted before landfall.
- NWS' Portland OR SOO (Bill Schneider) upgraded earlier Snow Advisory to a Winter Storm Warning based on this lower snow level.
- Forecasters' use of these data provided valuable lead time.

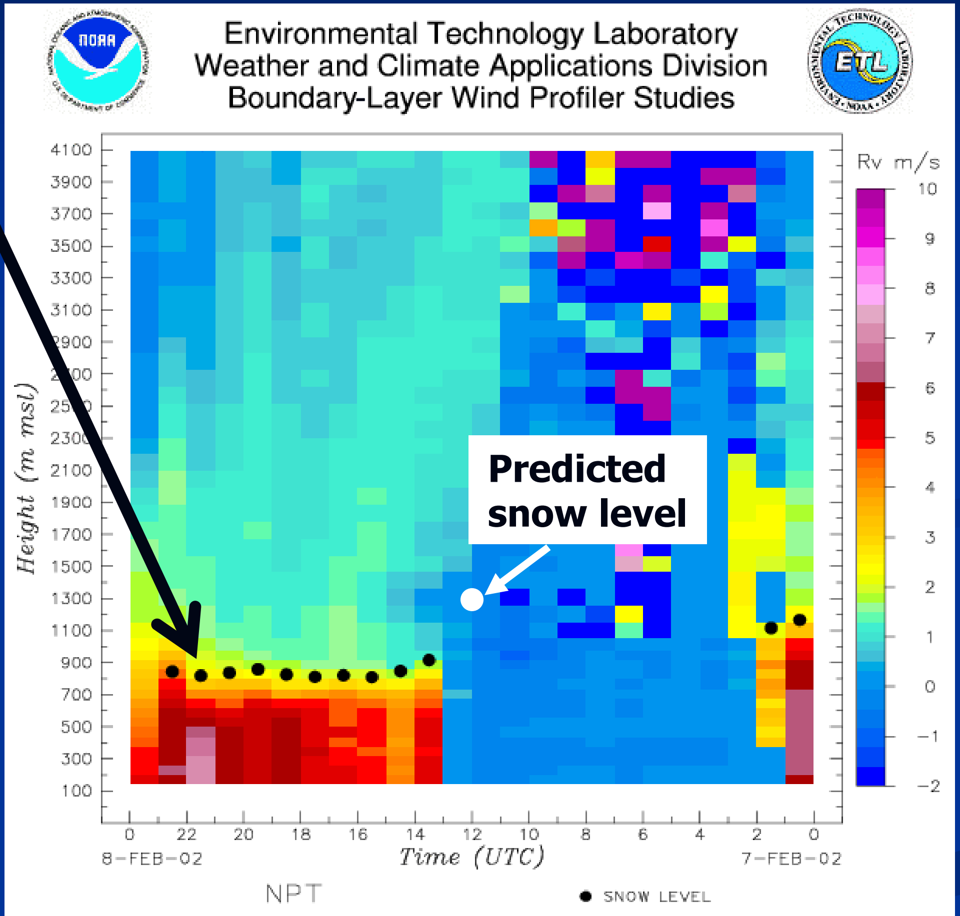

Time (UTC)	2330	2230	2130	2030	1930	1830	1730	1630	1530	1430	1330	1230
Snow Level (m)	none	843	818	836	858	825	811	820	809	847	915	none
Snow Level (ft)	none	2765	2683	2742	2814	2705	2660	2689	2653	2778	3001	none
Sfc Temp (C)	4.00	4.74	5.42	6.02	6.21	6.46	6.52	6.95	7.25	7.30	7.93	8.70

Operational Forecasting

Quotes from NWS forecasters collected during NOAA/ETL's profiler data usage surveys conducted by Dr. Louisa B. Nance*

[Re: wind profile data] "Ocean effect snow – profiler data showing much more northeasterly component to wind field in low levels and rather deep. Very, very helpful in maintaining snow forecast for cape/islands this morning given onshore flow." *(Boston, Jan. 18, 2003)*

[Re: Snow level product] "Very helpful! Showed the changeover from freezing rain to snow nicely." *(Binghamton, Dec. 12, 2002)*

[Re: RASS data] "Outstanding depiction of the structure of cold air daming erosion." *(NWS Eastern Region Headquarters, Sep. 27, 2002)*

[Re: Surface met data] Temperature, pressure, wind speed and direction all very useful for discerning southerly surge that is currently in progress! *(Monterey, Mar. 28, 2002)*

*See Poster 1.5 in CEIS, Tuesday AM

Operational Forecasting

"Need more profilers in northeast United States. Used by NWS to make forecasts."

Binghamton, NY WFO – August 1, 2002

New England Temperature and Air Quality Study

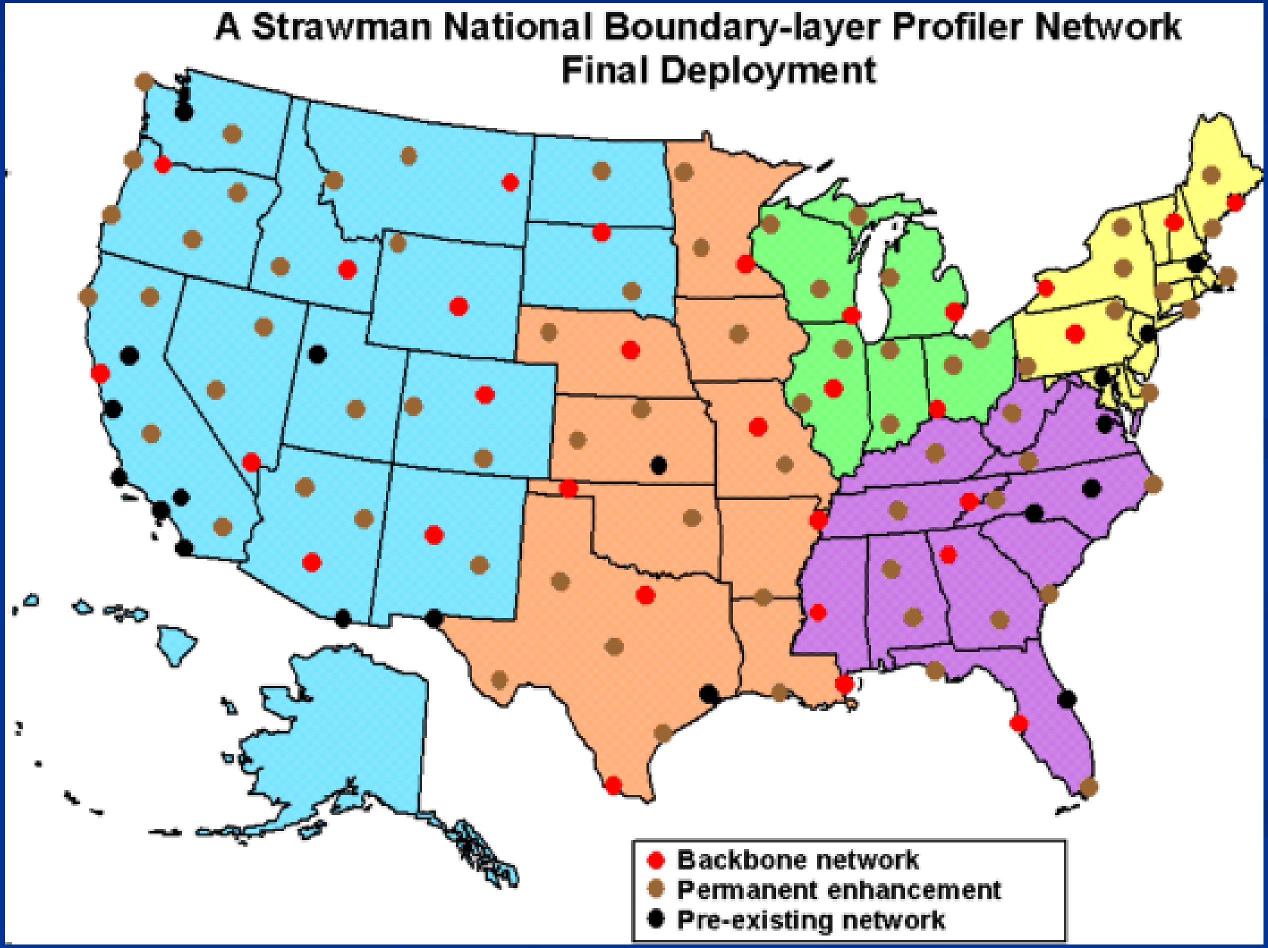

Operational Forecasting

Buoy-mounted wind profiler

- Coastal and marine weather prediction suffers from a relative sparseness of coastal and offshore observations.
- USWRP Report No. 2 noted that "the most serious gap in the current observing system for 1-5 day forecasts is the absence of wind profiles, especially over the northeast Pacific Ocean."
- BMWP technology is part of an FY05 initiative being considered by NOAA.

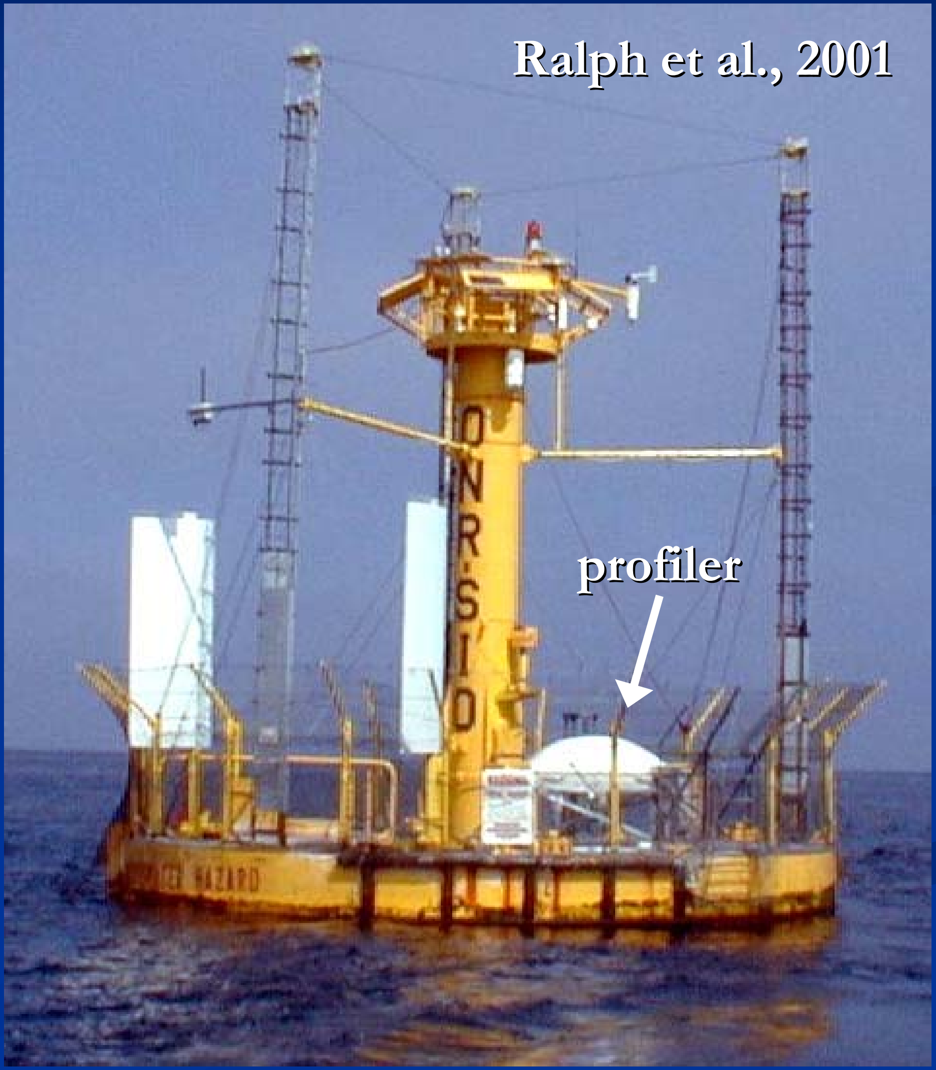

Bibliography

Gossard, E.E., et al., 1998: Measurement of clear-air gradients and turbulence properties with radar wind profilers. *J. Atmos. Oceanic Technol.*, 15, 321-342.

Gossard, E.E., 1990: Radar research on the atmospheric boundary layer. *Radar in Meteorology,* D. Atlas, Ed., AMS, Boston, 447-527.

Jacoby-Koaly, S., et al., 2002: Turbulent dissipation rate in the boundary layer via UHF wind profiler Doppler spectral width measurements. *Boundary-Layer Meteor.,* 103, 361-389.

Kaimal, J.C., et al., 1989: Effect of finite spectra on atmospheric turbulence. *Bound.-Layer Meteor.,* 47, 337-347.

Kristensen, L., 1971: The effect of aliasing, averaging and smoothing in digital spectrum analysis. *Statistical Methods and Instrumentation in Gophysics,* A.G. Kjelaas, Ed., Teknologisk Forlag, Oslo, 1-24.

Neff W.D., and R.L. Coulter, 1986: Acoustic remote sensing, in *Probing the Atmospheric Boundary Layer,* D.H. Lenschow, ed., AMS, Boston, 201-239.

Bibliography

Neiman, P.J. et al., 2002: The statistical relationship between upslope flow and rainfall in Clifornia's coastal mountains: Observations during CALJET. *Mon. Wea. Rev.,* 130, 1468-1492.

Ralph, F.M., et al., 2001: Buoy-mounted wind profiling: Current status and potential applications for coastal research and prediction. *4th Conf. on Coastal Atmos. and Oceanic Prediction and Processes*, 6-9 November, 2001, St. Petersburg, FL, AMS, Boston, 18-23.

Shaw, W.J., and J.M. Hubbe , 2000: A comparison of moments extracted from wind profiler spectra with in situ measurements. *Preprints, AMS 9th Conf. on Mountain Meteorology,* 7-11 August, 2000, Aspen, CO, AMS, Boston, 253-256.

White, A.B., 1997: Radar remote sensing of scalar and velocity microturbulence in the convective boundary layer. NOAA Tech. Memo. ERL ETL-276, Environmental Technology Laboratory, Boulder, CO, 127 pp.

White, A.B., et al., 1999: Space and time filtering of remotely sensed velocity turbulence. *J. Atmos. Oceanic Technol.,* 16, 1967-1972.

Bibliography

White, A.B., et al., 2002: An automated brightband height detection algorithm for use with Doppler radar spectral moments. *J. Atmos. Oceanic Technol.,* 19, 687-697.

Williams, C.R., 2002: Simultaneous ambient air motion and raindrop size distributions retrieved from UHF vertical incident profiler observations. *Radio Sci.*, 37, doi:10.1029/2000RS002603.

Wyngaard, J.C., 1992: Atmospheric Turbulence. *Annu. Rev. Fluid Mech.,* 24, 205-233.